



**US Army Corps
of Engineers**
Waterways Experiment
Station

Technical Report W-94-3
June 1994

HYDRAULICS LAB COPY

Water Quality Research Program

Destratification Induced by Bubble Plumes

*by Kreshimir Zic, Hienz G. Stefan
St. Anthony Falls Hydraulic Laboratory*

edited by Herman O. Turner, Steven C. Wilhelms

WES

Approved For Public Release; Distribution Is Unlimited

The contents of this report are not to be used for advertising, publication, or promotional purposes. Citation of trade names does not constitute an official endorsement or approval of the use of such commercial products.



PRINTED ON RECYCLED PAPER

Destratification Induced by Bubble Plumes

by Kreshimir Zic, Hienz G. Stefan

St. Anthony Falls Hydraulic Laboratory
Department of Civil and Mineral Engineering
University of Minnesota
3rd Avenue at Mississippi River, S.E.
Minneapolis, MN 55414

edited by Herman O. Turner, Steven C. Wilhelms

U.S. Army Corps of Engineers
Waterways Experiment Station
3909 Halls Ferry Road
Vicksburg, MS 39180-6199

Final report

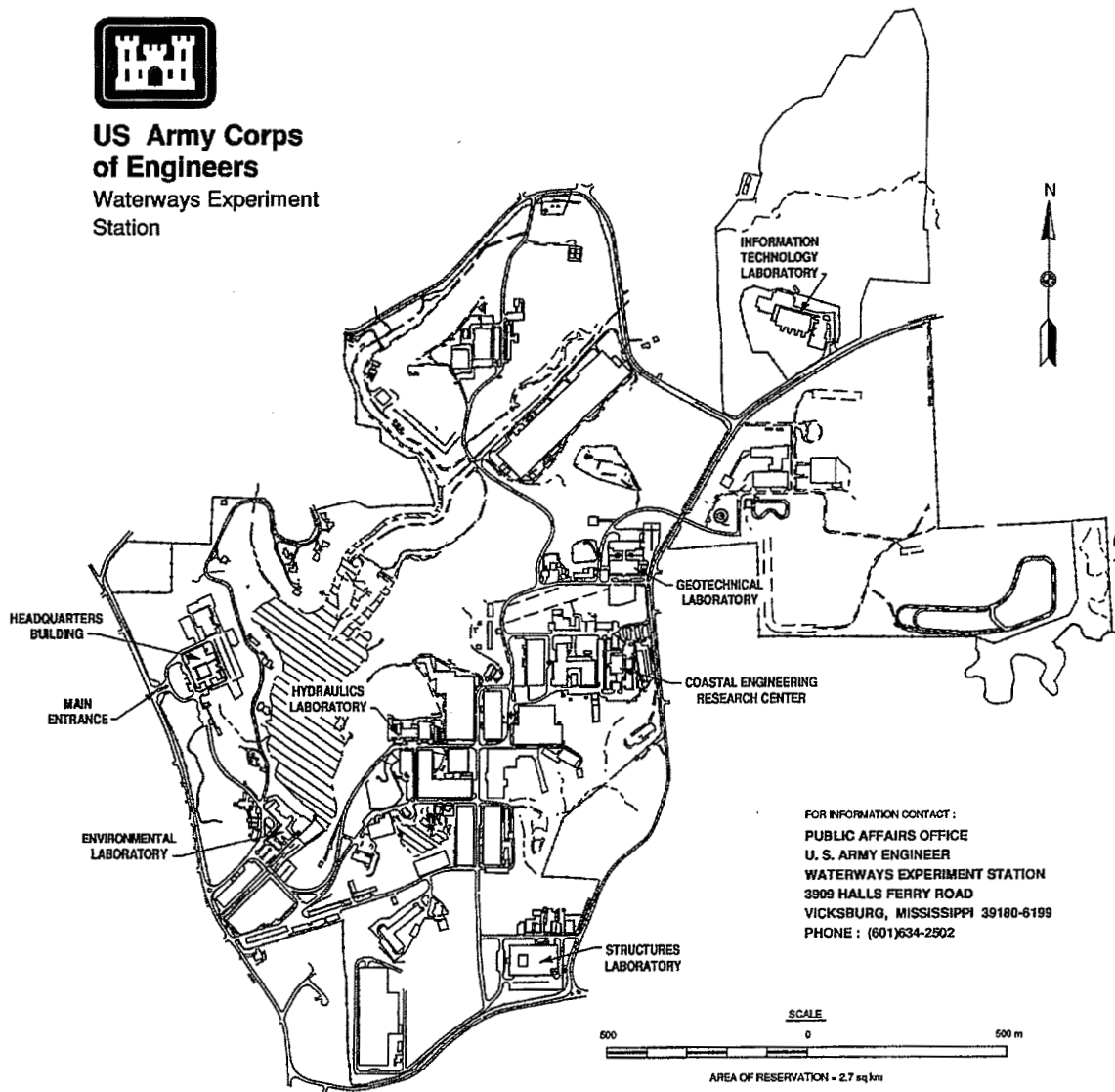
Approved for public release; distribution is unlimited

Prepared for U.S. Army Corps of Engineers
Washington, DC 20314-1000

Under WQRP Work Unit 32514



**US Army Corps
of Engineers**
Waterways Experiment
Station



Waterways Experiment Station Cataloging-in-Publication Data

Zic, Kreshimir.

Destratification induced by bubble plumes / by Kreshimir Zic, Heinz G. Stefan ; edited by Herman O. Turner, Steven C. Wilhelms ; prepared for U.S. Army Corps of Engineers.

54 p. : ill. ; 28 cm. -- (Technical report ; W-94-3)

Includes bibliographical references.

1. Reservoirs -- Destratification.
2. Lakes -- Destratification.
3. Plumes -- Fluid dynamics. I. Stefan, H. G. (Heinz G.) II. Turner, Herman O. III. Wilhelms, Steven C. IV. United States. Army. Corps of Engineers. V. U.S. Army Engineer Waterways Experiment Station. VI. Water Quality Research Program. VII. Title. VIII. Series: Technical report (U.S. Army Engineer Waterways Experiment Station) ; W-94-3. TA7 W34 no.W-94-3

Contents

Preface	v
Conversion Factors, Non-SI to SI Units of Measurement	vi
1—Introduction	1
Background	1
Objective and Scope	3
Physical Processes in Pneumatic Destratification	3
Past Research on Bubble Plumes	4
2—Mathematical Model Description	7
Near-Field Model	8
Bubble Plume	8
Surface Radial Jet	9
Mixing Regions	9
Transition from Near Field to Far Field	11
Far-Field Model	13
Analysis of Mixing Efficiency	15
3—Computer Program	16
Program Structure	16
Input Data Requirements	18
Incorporation into CE-THERM-R1	21
4—Model Validation	23
5—Summary	35
References	37
Appendix A: Bubble Plume Model by Poon (1985)	A1
Appendix B: Variables Used in Program BUBBLES	B1
Appendix C: Input Files Used for Simulation of Destratification	C1
Appendix D: Output File From Air Mixing Routine	D1

List of Figures

Figure 1.	Destratification systems	2
Figure 2.	Schematic presentation of the flow field as used in model formulation	4
Figure 3.	Schematic presentation of information flow	17
Figure 4.	General flowchart	18
Figure 5.	Flowchart for air mixing routine	19
Figure 6.	Notation used in air mixing routine	20
Figure 7.	Notation used in CE-QUAL-R1	20
Figure 8.	Sequence of CE-THERM elements and air mixing routine	22
Figure 9.	Simulation of destratification in laboratory experiment 8/04/88	24
Figure 10.	Simulation of destratification in laboratory experiment 8/05/88	25
Figure 11.	Simulation of destratification in laboratory experiment 8/08/88	26
Figure 12.	Simulation of destratification in laboratory experiment 8/10/88	27
Figure 13.	Simulation of destratification in laboratory experiment 8/16/88	28
Figure 14.	Simulation of destratification in laboratory experiment 8/17/88	29
Figure 15.	Bathymetric map of Lake Calhoun	31
Figure 16.	Calibration results for CE-QUAL-R1	32
Figure 17.	Simulation of destratification of Lake Calhoun	33

Preface

The work reported herein was conducted as part of the Water Quality Research Program (WQRP), Work Unit 32514. The WQRP is sponsored by the Headquarters, U.S. Army Corps of Engineers (HQUSACE), and is assigned to the U.S. Army Engineer Waterways Experiment Station (WES) under the purview of the Environmental Laboratory (EL). Funding was provided under Department of the Army Appropriation No. 96X3121, General Investigation. The WQRP is managed under the Environmental Resources Research and Assistance Programs (ERRAP), Mr. J. L. Decell, Manager. Mr. Robert C. Gunkel was Assistant Manager, ERRAP, for the WQRP. Technical Monitors during this study were Messrs. Frederick B. Juhle and Rixie Hardy and Dr. John Bushman, HQUSACE.

Under contract, Drs. Kreshimir Zic and Hienz G. Stefan, St. Anthony Falls Hydraulic Laboratory, Department of Civil and Mineral Engineering, University of Minnesota, developed the mathematical and numerical descriptions of destratification and the BUBBLES subroutine and prepared this report. The numerical model and the report were evaluated and edited by Messrs. Herman O. Turner and Steven C. Wilhelms, Reservoir Water Quality Branch (RWQB), Hydraulic Structures Division (HSD), Hydraulics Laboratory (HL), WES. Mr. Turner made minor modifications, improvements, and corrections to the computer code.

Work for the report was conducted during the period March 1990 through May 1993 under the direction of Mr. Frank A. Herrmann, Jr., Director, HL, and Mr. Glenn A. Pickering, Chief, HSD, and Acting Chief, RWQB. Mr. Pickering reviewed the report. Dr. John W. Keeley was Director, EL.

At the time of publication of this report, Director of WES was Dr. Robert W. Whalin. Commander was COL Bruce K. Howard, EN.

This report should be cited as follows:

Zic, K., and Stefan, H. G. (1994). "Destratification induced by bubble plumes," H. O. Turner and S. C. Wilhelms, ed., Technical Report W-94-3, U.S. Army Engineer Waterways Experiment Station, Vicksburg, MS.

Conversion Factors, Non-SI to SI Units of Measurement

Non-SI units of measurement used in this report can be converted to SI units as follows:

Multiply	By	To Obtain
feet	0.3048	meters
miles (U.S. statute)	1.609347	kilometers

1 Introduction

Background

Water bodies, such as lakes and reservoirs, experience seasonal temperature stratification with warmer water at the surface and colder water at the bottom. Temperature stratification is strongest during the late summer months because of the high incidence of solar radiation. This energy input warms the surface of the reservoir, causing large thermal gradients in the water body. The thermal gradients impede circulation and internal mixing and restrict the transport of oxygen from the surface layers to the bottom.

As a consequence, the cold water (hypolimnion) deep in the reservoir becomes isolated from the warmer surface water (epilimnion). Biochemical processes in the reservoir water and at the reservoir bottom use oxygen. Because oxygen is not transported to the hypolimnion from the epilimnion, low oxygen concentrations or even anaerobic conditions are created at these lower depths. Under anaerobic conditions, water quality suffers because of trace metal dissolution, nutrient release that stimulates eutrophication, production of hydrogen sulfide gas, and a lowering of the pH.

Destratification, as its name implies, has the objective of disrupting thermal stratification to allow natural processes to improve the quality of the lake. The induced mixing and circulation acts to cool the epilimnion and warm the hypolimnion, resulting in a more uniform temperature profile throughout the water column. Destratification of a lake or reservoir eliminates or minimizes the undesirable anaerobic conditions of the lower layers by mixing the hypolimnion and epilimnion and exposing the water to the surface where oxygen absorption occurs.

A destratification system operates by adding energy to the water body through an artificial means to destratify the lake or reservoir. Depending upon its specific character, usually, a destratification system results in the cyclical mixing of the water column (Figure 1). The induced circulation brings the cooler, oxygen-deficient bottom water to the surface where reaeration occurs. The warmer, oxygen-rich surface waters are entrained and displaced to the lower depths causing an increase in the temperature and dissolved-oxygen content of the bottom water.

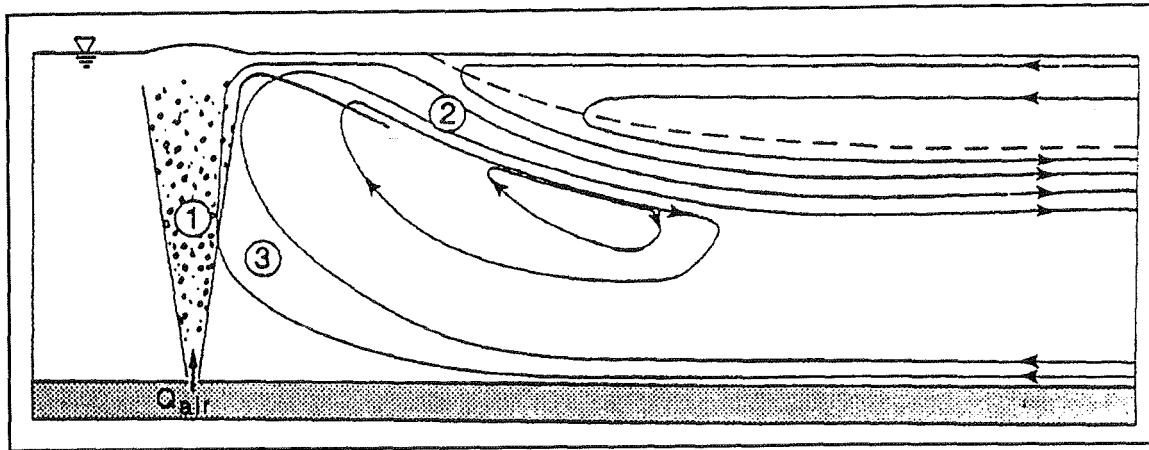


Figure 1. Destratification systems

The two types of destratification systems used are classified as hydraulic or pneumatic devices. The hydraulic systems pump water as the mechanism for imparting the energy to the reservoir for destratification. Axial flow pumps or direct drive mixers are examples of hydraulic destratification systems (Price 1988; Punnett 1991). These axial flow pumps generate a low-velocity jet by rotating a large-diameter propeller (6- to 15-ft) at slow speed.¹ On the other hand, the direct drive mixers generate a high-velocity jet by rotating a small-diameter propeller (1- to 2-ft) at high speed. The axial flow pumps generate a high discharge because of the large diameter propeller; however, the flow is at low velocity. The direct drive mixers produce a high-velocity jet; therefore, they add more momentum to the jet, but must rely on entrainment to increase the pumped volume of water.

Pneumatic systems operate by introducing a continuous stream of air bubbles to the water column. As the air is released, a bubble plume is formed consisting of air bubbles and entrained water. The bubble plume creates a flow of water from the hypolimnion to the surface. When the bubble plume reaches the surface, the entrained hypolimnetic water spreads horizontally until density causes it to plunge to a region of neutral density. This cycle continues until the density difference of the water column above the diffuser is essentially zero. Occasional operation of the pneumatic diffuser after uniform density is reached maintains a destratified condition by continually disrupting newly established stratification in the reservoir.

Pneumatic systems are usually composed of three parts: an onshore air compressor, supply line, and a diffuser system. Diffuser systems may be point source or line source. A line source diffuser is often fabricated by drilling holes in a pipe that permits air to escape. This type of diffuser allows the bubble plume to form vertical recirculation cells on either side of the line diffuser. A point source diffuser releases air at essentially a single point along the supply line and forms a radial circulation pattern.

¹ A table of factors for converting non-SI units of measurement to SI units is presented on page vi.

Objective and Scope

The physical and limnological effects of destratification are fairly well understood and describable in general terms (Pastorok, Lovenzen, and Ginn 1982). However, guidance for designing a pneumatic destratification system is limited with many generalizations that may not be applicable at all Corps of Engineers reservoirs. No methodology exists to examine the long-term operation of a destratification system.

The objective of this report is to explain the concepts of pneumatic destratification and the basis for incorporating these concepts into the one-dimensional numerical model CE-THERM-R1, which is the thermal module within the water quality model CE-QUAL-R1 (Environmental Laboratory 1982). By coupling a numerical description of destratification and CE-THERM-R1, long-term effects of reservoir destratification can be investigated. Topics covered in this report include conceptual and theoretical descriptions of pneumatic destratification, description of the destratification option in CE-THERM-R1, and comparison of laboratory and field observations with model predictions.

Physical Processes in Pneumatic Destratification

Pneumatic destratification of a water body is a process whereby air is injected near the bottom of a water body to overcome and disrupt its natural thermal stratification. Simply stated, air is injected through a diffuser¹ near the bottom, and the bubbles rise to the surface causing mixing. When the bubbles exit the diffuser, a bubble plume is formed that drags hypolimnetic water along with it. As the plume rises, it continues to entrain the colder water in the hypolimnion. Water from the metalimnion and epilimnion are also entrained before the plume reaches the surface. The water that is pumped by the bubble plume spreads out at the surface and mixes with the warmer, less dense surface water. Spreading continues until the mixed water plunges because of density to seek a neutral density layer (Figure 2). These processes continue until, ultimately, the stratification is destroyed.

In continuous operation, the bubble plume causes circulation cells to form. As mentioned, for a linear diffuser, these cells are formed along each side of the bubble plume. For a point source diffuser, circulation cells are formed radially (Figure 1). These mixing cells are highly unstable regions and provide an avenue where natural processes, such as wind mixing and diurnal cooling, can aid in the disruption of thermal stratification.

¹ For introductory purposes, a diffuser is any type of air outlet device.

Past Research on Bubble Plumes

Air bubble plumes have been the subject of many studies (Kobus 1968, 1973; Tekeli and Maxwell 1978; Cederwall and Ditmars 1970; Milgram 1983; Tsang 1984; Rowe, Poon, and Lareshen 1989). Mostly plume mechanics, i.e., air-water interaction, gas-exchange, and bubble mechanics were of main interests. Only a few investigators (Graham 1978; McDougall 1978; Goossens 1979; Kranenburg 1979; Hossain and Narang 1983; Asaeda and Imberger 1988; Patterson and Imberger 1989) analyzed the interaction of air bubble plumes with density stratified environments.

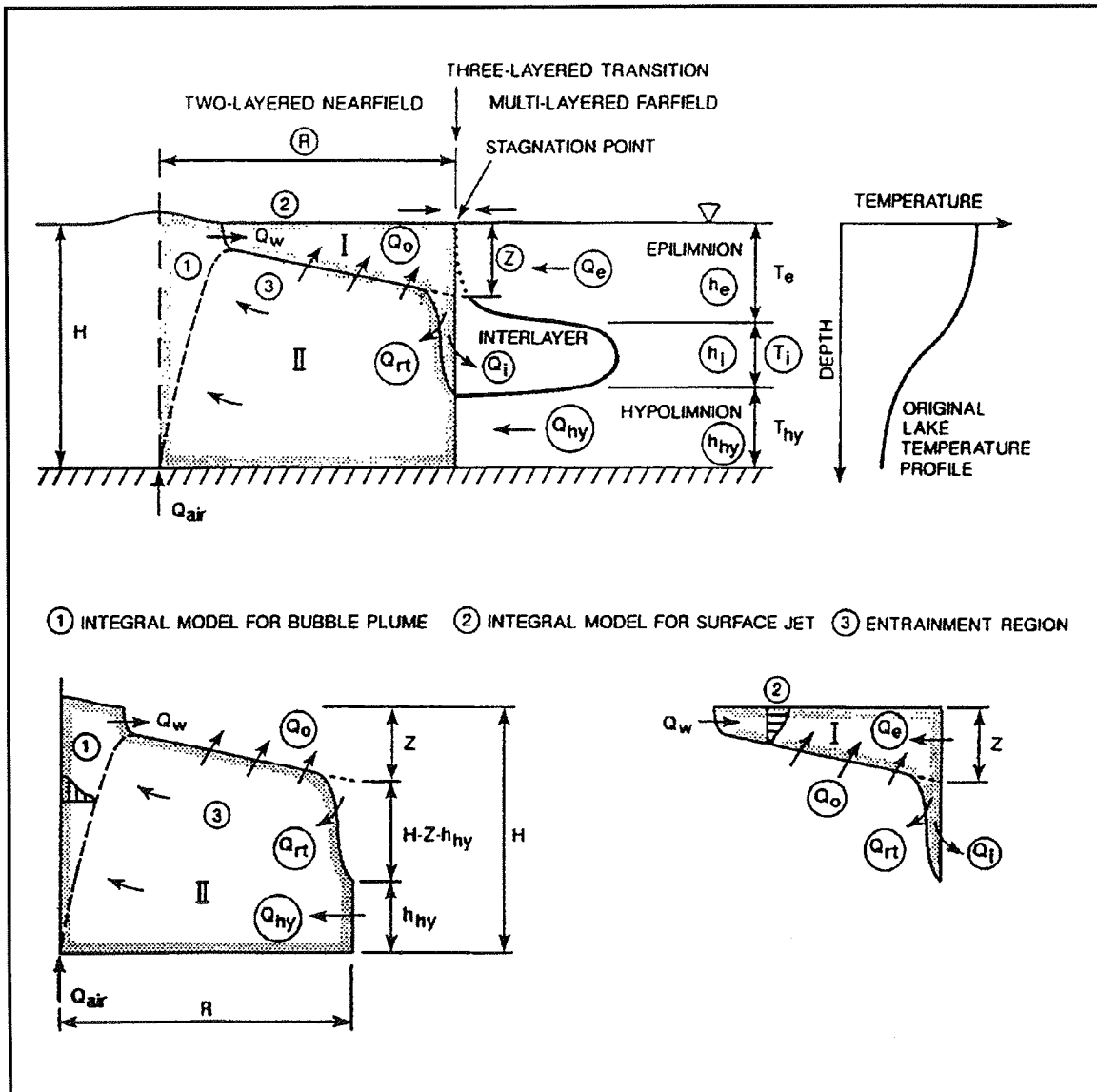


Figure 2. Schematic presentation of the flow field as used in model formulation (Zic and Stefan 1990)

Asaeda and Imberger (1988) described three types of interaction between a bubble plume and a linearly stratified environment and two types for a two-layered stratification. The interaction then depends on a bubble plume number introduced by Asaeda and Imberger (1988) for two-layer systems

$$P \Delta = \frac{(g')^{1.5} h_l^{1.5} H}{g Q_{air}} \left(\frac{h_u}{H} \right)^3 \quad (1)$$

and for a linearly stratified system

$$P N = \frac{N^3 H^4}{g Q_{air}} \quad (2)$$

where

g' = a reduced acceleration because of gravity = $g \Delta \rho / \rho_r$

$\Delta \rho$ = density difference between the two layers

ρ_r = reference density

g = acceleration because of gravity

h_l = thickness of lower layer

h_u = thickness of upper layer

H = submergence depth of diffuser

Q_{air} = gas release rate at atmospheric conditions

N = buoyancy frequency = $(-g \rho_r^{-1} d \rho_a / d a)^{0.5}$

ρ_a = ambient density

According to Asaeda and Imberger (1988), the vertical flow of water induced by the bubble plume impinges at the interface of the two-layered stratification, and a horizontal intrusion occurs at the interface when $P \Delta > 30$. This is the case of a very strong stratification and a weak bubble plume. For $P \Delta < 30$, the strong bubble-plume-induced flow in a weakly stratified water column breaks through the interface and an air-water mixture reaches the free surface, where it spreads horizontally and plunges after some distance. When the plunging flow reaches the depth of the neutral buoyancy relative to its density, it spreads horizontally. The first regime was observed in the laboratory with a strong stratification obtained with salt (McDougall 1978; Asaeda and Imberger 1988). In a linearly stratified fluid, three well-defined regions of the flow were evident: the moving flow core consisting of a mixture of air bubble bubbles and dense fluid, an annular downdraft, and beyond that, the intrusion flows. At very large gas flow rates, a single intrusion was observed. As the flow rate was decreased, the buoyancy flux was insufficient to carry lower fluid to the surface; multiple intrusions were observed exiting the downdraft region at

equally spaced elevations. At very low gas flow rates, the intrusions became unsteady and much less well defined. The values of Pn number for the first regime were less than 300, for the second $300 < Pn < 1,000$, and $Pn > 1,000$ for the third regime. In practical applications of the bubble plume as a lake destratification device, the bubble plume numbers are typically less than 1.0 (Tables 1 and 2), and the bubble plume effect is very strong relative to the density stratification. Direct observations of the flow field were made by Goossens (1979) in a field study and by Zic, Stefan, and Ellis (1989) in a laboratory study with a thermal stratification. A typical flow pattern (streamlines) is shown in Figure 1.

Lake	H , m	H_1 , m	g' , ms^{-2}	Q_{air} , m^3s^{-1}	$P\Delta$	Source
Calhoun	19.0	9.0	0.023	0.059	0.50	Shapiro and Pfannkuch 1973
Petrusplaat-1978	15.0	8.0	0.012	0.17	0.03	Goossens 1979
Maarsseveen	18.9	9.8	0.019	0.042	0.41	Knoppert et al. 1970

Lake	H , m	g' , ms^{-2}	Q_{air} , m^3s^{-1}	PN	Source
Ikari	28.0	0.025	0.077	0.36	Ito 1972
Shikazawa	9.0	0.013	0.077	0.02	Ito 1972
Petrusplaat-1977	15.0	0.01	0.170	0.24	Goossens 1979

The most common approach to bubble plume analysis is the use of integral models (Kobus 1968, 1973; McDougall 1978; Milgram 1983). Goossens (1979) proposed a composite model to analyze the effects of an air bubble plume on lake stratification. Zic and Stefan (1988) improved Goossens' (1979) near-field model and combined it with a dynamic lake temperature stratification model MINLAKE (Stefan and Ford 1975; Ford and Stefan 1980; Riley and Stefan 1987, 1988). Patterson and Imberger (1989) combined McDougall's (1978) bubble plume model with a dynamic reservoir simulation model DYRESM (Imberger and Patterson 1981). Both approaches allow the simulation of stratification changes in lakes or reservoirs over the period when an air bubble system operates.

2 Mathematical Model Description

As described earlier, if air is injected from the bottom of a two-layered stratified environment, where the warmer and lighter water at the surface is called epilimnion and the colder and heavier water below hypolimnion, water with high density from the hypolimnion will be brought to the surface. This heavier water flows off and collides with the lighter epilimnion water. So the heavy water will pass (plunge) under the epilimnion and spread as an intermediate layer (Figure 1). Experimental evidence of this interflow was provided by Kranenburg (1979), Goossens (1979), and Zic, Stefan, and Ellis (1989). Since there is mixing between discharged and epilimnetic water, the interflow density is intermediate between the epilimnion and hypolimnion densities. In the far field, this produces a new layer since density differences suppress turbulence and mixing at the boundaries. But near the stagnation (plunging) area, higher turbulence provides some mixing (Goossens 1979).

A simplified flow pattern under stratified conditions is shown in Figure 1. The major characteristics of the flow are the eddy-like motion in the vicinity of the air release and a three-layer flow in the region further away from the bubble plume. Goossens (1979) and Zic (1990) established that there is no significant difference between the flow pattern for isothermal and stratified receiving water in the vicinity of an air bubble plume. It is the density difference between the epilimnion and hypolimnion that influences the flow pattern. The plunging of the surface radial jet is governed by the interaction between the buoyancy force and momentum of the flow. Accordingly, the greater density difference causes bigger negative buoyancy of the surface radial jet and earlier plunging. Increase of the air release rate by a small amount will not change the momentum of the flow significantly. Therefore, it will not greatly affect the position of the plunging point, but the flow rates in the three layers will be affected (Goossens 1979). The thickness of the epilimnion affects the density of the interflow (mixing) layer flowing into the lake. A thicker epilimnion decreases the mixing layer density, which then slides over the denser hypolimnetic water. A thin epilimnion, on the other hand, provides for a heavier mixing layer that mixes with the hypolimnion more easily.

The mathematical model of the air bubble column and near- and far-field circulation is based on the model developed by Goossens (1979). The model characterizes the mixing of a bubble plume with two regions in the lake (Figure 2):

- a. A region near the air bubble column, which is treated as a two-layer system and called the near field.
- b. The bulk (remainder) of the lake, which is treated as a multilayered temperature (density) stratified environment and called the far field.

The boundary between the two regions is set through the stagnation point (plunge point) of the horizontal surface flow away from the plume (Figure 2).

Near-Field Model

The near field consists of four main regions also shown in Figure 2:

- a. A plume of water induced by air bubbles (marked as I).
- b. A horizontal surface jet, which begins where the upward flow induced by the bubbles is deflected by the water surface and which plunges into the surroundings because it is negatively buoyant (marked as II).
- c. Two mixing regions in which ambient water is drawn toward the bubble plume and entrained by it (marked as I and II).
- d. Transition from near field to far field at the stagnation point.

Bubble Plume

The bubble plume is analyzed as a two-phase buoyant plume analogous to a single-phase buoyant plume. Its entrainment coefficient is equal or slightly greater than that of a single-phase plume (Goossens 1979). The ambient stratification is assumed not to have an influence on the plume development. If the expansion of the air is adiabatic and supported by measurements in the laboratory and in the field, the following relation between the submergence depth of diffuser H , the volumetric gas rate at atmospheric pressure Q_{air} , and the volumetric outflow rate from the bubble plume at the surface Q_w was obtained (Goossens 1979)

$$Q_w = 0.47 H^{4/3} Q_{air}^{1/3} \quad (3)$$

Surface Radial Jet

Once the plume reaches the surface, it starts to spread horizontally. The assumptions under which the mathematical model was developed are the following: (a) isothermal ambient water, (b) stationary conditions with radial symmetry, (c) no Coriolis force influence, and (d) a sufficiently turbulent flow to neglect viscous effects.

The Navier Stokes equations can be solved assuming a similarity for the velocity and shear stress profiles. Regardless of the reservoir depth, the assumption is made that the hypolimnetic flow toward a bubble plume has no influence on the velocity profile of the surface jet. The solution, in terms of the total surface flow at the stagnation point ($r = R$), is (Goossens 1979)

$$Q_o + Q_w = 2 \pi m R \left[\tanh\left(\frac{Z}{kR}\right) - \frac{Z}{H} \tanh\left(\frac{H}{kH}\right) \right] \quad (4)$$

with a jet thickness

$$Z = kR \tanh^{-1} \left[\sqrt{1 - \frac{kR}{H} \tanh\left(\frac{H}{kR}\right)} \right] \quad (5)$$

where

$$m = 0.69 k^{0.5} Q^{0.35} H^{0.5}$$

$$k = 0.0725 (Q_{air} \text{ in } m^3/s, H \text{ in } m)$$

Q_o = flow rate of water entrained by the radial surface jet

Mixing Regions

Mixing zone I entrains the discharge from the vertical plume (Q_w), from the radial surface jet (Q_o), and from the epilimnion (Q_e) and yields the return flow (Q_{ri}) to the mixing zone II and the interlayer flow (Q_j) to the far field. Mixing zone II entrains hypolimnetic water (Q_{hy}) and return flow (Q_{ri}) and yields a discharge ($Q_w + Q_o$) to mixing zone I. The mass balances of mixing zones I and II yield expressions for the interlayer density ρ_i and the density of the outflowing discharge at the surface ρ_o (Figure 2)

$$(Q_w + Q_o + Q_e) \rho_i = (Q_w + Q_o) \rho_o + Q_e \rho_e \quad (6)$$

$$(Q_w + Q_o) \rho_o = (Q_w + Q_o + Q_{hy}) \rho_i + Q_{hy} \rho_{hy} \quad (7)$$

where ρ_e and ρ_{hy} are the epilimnion and hypolimnion densities, respectively. Based on Equations 6 and 7, the interlayer density ρ_i is equal to (Goossens 1979)

$$\rho_i = \frac{Q_e \rho_e + Q_{hy} \rho_{hy}}{Q_e + Q_{hy}} \quad (8)$$

From the experimental data for nonseparated plunging flows with a sloping bottom (Johnson, Ellis, and Stefan 1989), it can be derived that the entrainment velocity at the position of plunging is 30 percent of the mean velocity at the plunging point.

$$Q_e = 0.3 \frac{h_e}{Z} (Q_w + Q_o) \quad (9)$$

It has been found in experiments (Zic, Stefan, and Ellis 1989) that the entrainment from the hypolimnion is not affected by the ambient stratification and corresponds to the entrainment obtained under similar conditions in isothermal water. Accordingly, the relationship $Q_{hy} = f(Q_{air}, H, h_{hy})$ can be closed using the results obtained under isothermal conditions. For convenience, the relationship by Kobus (1973) is used here and rewritten as

$$Q_{hy} = Q_{air}^{0.1} \sqrt[3]{\frac{g H_o^5}{Q_{air}^2}} \left[\text{Tanh} \left(\frac{\sqrt[3]{g Q_{air} / H_o}}{\Delta u_b} \right) \right]^{1/2} \quad (10)$$

$$\left(\frac{H + H_o}{H_o} \right)^{4/3} \left[\frac{(h^* + 0.05)^5}{(1 - h^*)} \right]^{1/3} \quad (11)$$

$$h^* = \frac{h_{hy}}{h_{hy} + H}$$

where

$$H_o = 10.0 \text{ m}$$

$$\Delta u_b = \text{relative bubble velocity} = 0.25 \text{ m/sec}$$

The Kobus' model was developed based on experimental conditions with air flow rates below $0.001 \text{ m}^3/\text{sec}$. For air flow rates higher than $0.001 \text{ m}^3/\text{sec}$, a model by Poon (1985) was used. It has been found to perform better for the higher air flow rates than the Kobus (1973) model (Zic 1990). The equations used in the Poon (1985) model are presented in Appendix A.

Transition from Near Field to Far Field

The horizontal extent of the mixing regions as characterized by the location of the stagnation point can be determined by assuming equilibrium between near-field (F^n) and far-field (F^f) forces (Goossens 1979)

$$F^n = F^f \quad (12)$$

at $r = R$. Each of these forces consists of a dynamic part (resulting from the water flow) and a static part (resulting from the water density). The dynamic part is, however, significantly smaller than the static one (Goossens 1979). The assumption was made that the stratification in the near field can be described as a two-layer system, obtained from the original temperature profile in the lake, with thicknesses h_{eo} and h_{hyo} for epilimnion and hypolimnion, respectively (Figure 2). The position of these two thicknesses is defined by a steepest gradient of the water temperature profile (midpoint of the thermocline). It has been found in simulations that the model is not sensitive to this assumption. At the end of the time step, the initial thicknesses h_{eo} and h_{hyo} will change to some new values h_e and h_{hy} at the point of transition to the far field. Accordingly, the near-field force can be written as

$$F^n = 2 \pi R g \left\{ 0.5 \rho_o Z^2 + \left[\rho_o Z + 0.5 \rho_i (H - h_{hyo} - Z) \right] (H - h_{hyo} - Z) + \left[\rho_o Z + \rho_i (H - h_{hyo} - Z) + 0.5 \rho_{hy} h_{hyo} \right] h_{hyo} \right\} \quad (13)$$

The far-field force is given as

$$F^f = 2 \pi R g \left\{ 0.5 \rho_o h_e^2 + \left[\rho_e h_e + 0.5 \rho_i h_i \right] h_i + \left[\rho_e h_e + \rho_i h_i + 0.5 \rho_{hy} h_{hy} \right] h_{hy} \right\} \quad (14)$$

where h_i = thickness of the interlayer at the transition to far field at the end of the time step (Figure 2). Substituting Equations 13 and 14 into Equation 12 allows a solution of the stagnation point distance R . The only unknowns remaining are (a) the thicknesses of the epilimnion h_e and (b) the thickness of the hypolimnion h_{hy} in the transition to the far field. If it is assumed that the mixing layer is located at the position that would result from a direct mixing of the appropriate epilimnion and hypolimnion flows, then (Goossens 1979)

$$h_e = h_{eo} - \frac{\rho_{hy} - \rho_i}{\rho_{hy} - \rho_e} h_i \quad (15)$$

$$h_{hy} = h_{hyo} - \frac{\rho_i - \rho_e}{\rho_{hy} - \rho_e} h_i \quad (16)$$

and from the lake geometry

$$H = h_{hyo} + h_{eo} = h_e + h_i + h_{hy} \quad (17)$$

the thickness of the interlayer h_i in the transition to the far field. Kranenburg (1979) compared the diving of the interlayer underneath the epilimnion with an open channel flow over a broadcrested weir. In this case, the epilimnion corresponded to the weir, and the mixing region in the near field corresponded to the hydraulic jump in front of it. At the transition R , there is critical flow if the far-field flow in the interlayer does not influence the flow at the transition. The condition for the presence of the critical flow is (Goossens 1979)

$$\begin{aligned} F_e^2 F_1^2 + F_1^2 F_{hy}^2 + F_{hy}^2 F_e^2 - \frac{\rho_{hy} - \rho_i}{\rho_{hy}} F_e^2 - \frac{\rho_{hy} - \rho_e}{\rho_{hy}} F_1^2 \\ - \frac{\rho_i - \rho_e}{\rho_{hy}} F_{hy}^2 + \frac{(\rho_i - \rho_e)(\rho_{hy} - \rho_i)}{\rho_{hy}^2} = 0 \end{aligned} \quad (18)$$

where the densimetric Froude numbers in the epilimnion (F_e), interlayer (F_1), and hypolimnion (F_{hy}) are defined, respectively, as

$$\begin{aligned} F_e &= \frac{1}{(2\pi R)^2} \frac{\rho_{hy} Q_e^2}{(\rho_{hy} - \rho_e) g h_e^3} \\ F_i &= \frac{1}{(2\pi R)^2} \frac{\rho_{hy} Q_1^2}{(\rho_{hy} - \rho_e) g h_1^3} \\ F_{hy} &= \frac{1}{(2\pi R)^2} \frac{\rho_{hy} Q_{hy}^2}{(\rho_{hy} - \rho_e) g h_{hy}^3} \end{aligned} \quad (19)$$

where the interlayer flow Q_i is equal to

$$Q_i = Q_{hy} + Q_e \quad (20)$$

The near-field model described above is for axisymmetric flow. The horizontal extent of the near field is usually less than 1 to 2 lake depths from the air injection point, as observed in a field study (Goossens 1979) and experiments (Zic, Stefan, and Ellis 1989).

The above model of the near field considers the most basic hydraulic phenomena. The input values are the initial temperature profile in the lake that must be transformed into a two-layer system and the volumetric air release rate Q_{air} . Outputs of the near-field model are the depths and the flow rates from the hypolimnion and the epilimnion, and the position, thickness, and the flow rate of the interlayer (Figure 2). The flow in the epilimnion and the hypolimnion is toward the air bubble column, and the flow in the interlayer is from the air bubble column toward the lake (far field).

Differences between the original Goossens' (1979) model and the one presented here are as follows:

- a. The near-field process is treated as unsteady, whereas a steady-state assumption was made by Goossens.
- b. Entrainment rate from the epilimnion, specified by the Equation 9, is obtained from the description of plunging flows by Johnson, Ellis, and Stefan (1989). Therefore, there is no need to obtain the epilimnetic entrainment in an iteration loop as proposed originally with a criterion that does not have a general applicability, but arose from limited model verification.
- c. Use of the equation (11) for the hypolimnetic entrainment overcomes a weak point of the original model: in the calculation of the return flow, the entrainment coefficient could vary from 1.0 to 8.0 (Goossens 1979): Experiments by Zic, Ellis, and Stefan (1989) showed that this coefficient could be as large as 14.0 and that the return flow was not related to the hypolimnetic flow.
- d. Entrainment of water from below the diffuser is included in the model (after Zic, Ellis, and Stefan 1989).

A preliminary version of the model was presented by Zic and Stefan (1988). Since then, laboratory experiments were performed to verify that the basic assumptions of the mixing model are physically realistic (Zic, Ellis, and Stefan 1989). The final version is described by Zic and Stefan (1990).

Far-Field Model

Once the near-field model calculates the flow rates and thicknesses at the transition point for a given time step, this information is used to calculate the change of the temperature profile in the far field. The multilayered far field consists of N horizontally homogeneous layers with different thicknesses (in general), where $T_{j,k}$ and $V_{j,k}$ are the water temperature and the volume of the layer j at the end of the time step k , respectively. Flow rates Q_e , Q_{hy} , and Q_i are assumed to be uniformly distributed over the

thicknesses h_e , h_{hy} , and h_i , respectively, giving the flow rate Q at each layer j . The entrainment from the epilimnion and the hypolimnion Q_e and Q_{hy} , respectively, reduces the volume, whereas the interlayer flow Q_i increases the volume of the layers affected. Therefore, in the epilimnion and hypolimnion (defined with h_e and h_{hy})

$$V_{j,k+1} = V_{j,k} - Q_j (t_{k+1} - t_k) \quad (21)$$

and in interlayer (defined with h_i)

$$V_{j,k+1} = V_{j,k} + Q_j (t_{k+1} - t_k) \quad (22)$$

The temperature of the interlayer flow $T_{i,k+1}$ is calculated based on the temperature of the layers from which the water has been entrained ($Q_j < 0$) as

$$T_{i,k+1} = \frac{\sum_{j=1}^{j+n} \left[T_{i,k+1} (Q_1 + Q_2 + \dots + Q_{j-1}) + T_{j,k} Q_j \right]}{(Q_1 + Q_2 + \dots + Q_j)} \quad (23)$$

The new temperature in the layers receiving the interlayer flow (defined with h_i) is the volume average of the temperature at the beginning of the time step and the interlayer temperature

$$T_{j,k+1} = \left[T_{j,k} V_{j,k} + T_{i,k+1} Q_j (t_{k+1} - t_k) \right] \frac{1}{V_{j,k+1}} \quad (24)$$

At the end of the time step t_{k+i} , the thicknesses of the far-field layers will be updated resulting from the changes in the volumes.

The same equations (from Equation 21 to Equation 24) are valid for the evaluation of mixing of any other dissolved substance in the water body, such as dissolved oxygen, that may be of interest in a given application in addition to water temperature.

The vertical diffusion occurring from the water flow in the far field is calculated using a one-dimensional diffusion equation

$$A \frac{\partial T}{\partial t} = \frac{\partial}{\partial z} K A \frac{\partial T}{\partial z} \quad (25)$$

where

K = vertical diffusion coefficient = 1×10^{-5} m²/sec (Goossens 1979)

A = surface area of a layer (from bathymetric map)

z = vertical coordinate

Analysis of Mixing Efficiency

A stability parameter S is commonly used in the analysis of the stratified lakes/reservoirs (Dortch 1979; Davis 1980; Patterson and Imberger 1989) and represents the difference between the potential energy of the stratified and well-mixed water body, given as (Ditmars 1970)

$$S = \rho g V_R (H - Y) \quad (26)$$

where

ρ = density of water

g = acceleration because of gravity

V_R = reservoir volume

H and Y are the center of mass for isothermal and stratified lake or reservoir, respectively, given as

$$H = \frac{\sum_{j=1}^{j=N} h_j V_j}{\sum_{j=1}^{j=N} V_j} ; Y = \frac{\sum_{j=1}^{j=N} \rho_j h_j V_j}{\sum_{j=1}^{j=N} \rho_j V_j} \quad (27)$$

where

ρ_j = density of the layer j

h_j = height to the centroid of each layer j above the bed of the reservoir

The stability parameter gives information about the energy content in the lake that interacts with the energy of the mixing device. Accordingly, the mixing efficiency can be calculated from the change of the stability of the lake (Dortch 1979; Patterson and Imberger 1989). Here, the effect of the air mixing device is evaluated using the percentage of mixing achieved, defined as

$$P = \frac{S_o - S_t}{S_o} \times 100 \quad (28)$$

where

S_o = initial stability

S_t = stability at time t

3 Computer Program

Program Structure

A computer program called BUBBLES was written to simulate the near field, the three-layer flow from the near field into the far field, and the change of the water quality parameters in the far field.

Since a lake or reservoir is also exposed to processes other than air plume mixing, the program BUBBLES is merged with a general dynamic lake stratification model: CE-THERM-R1 (Environmental Laboratory 1982). Merging BUBBLES with such a model produces a program that combines artificial lake mixing by air bubble diffusers with the naturally occurring stratification by heating, wind mixing, and natural convection by cooling. The program can, therefore, be used to determine air requirements to maintain or produce a fully mixed lake.

The information flow in the combined program is shown schematically in Figure 3. BUBBLES and CE-THERM-R1 are applied sequentially. The general flowchart and interaction between the main program and air mixing routine is shown in Figure 4. The flowchart for the air mixing routine is shown in Figure 5. It is important to emphasize that the bulk of the air mixing routine is independent from the main program. The computational procedure is organized such that the routine TRANSF transforms the geometry and temperature profile from the main program to the geometry and notation used in the air mixing routine, shown in Figure 6. The subroutine TWOLAY transforms the reservoir into a two-layer system from the original temperature profile. The position of these two layers is defined by the midpoint of the thermocline. The subroutine NEARF calculates the thicknesses and flow rates in the epilimnion, interlayer, and hypolimnion at the transition point to the far field. This information is used by the subroutine FARF, which updates the water quality parameters for a given computational step as defined in DTINSIM. Percentage of mixing is calculated in STABMX as the change of the stability over time. The variable NDAYC represents the number of the time steps elapsed. Initial stability (for NDAYC = 0) is STAB0. The last step in the computational loop for a given time step is the transformation of the temperature profile back to the notation and geometry used in the main program

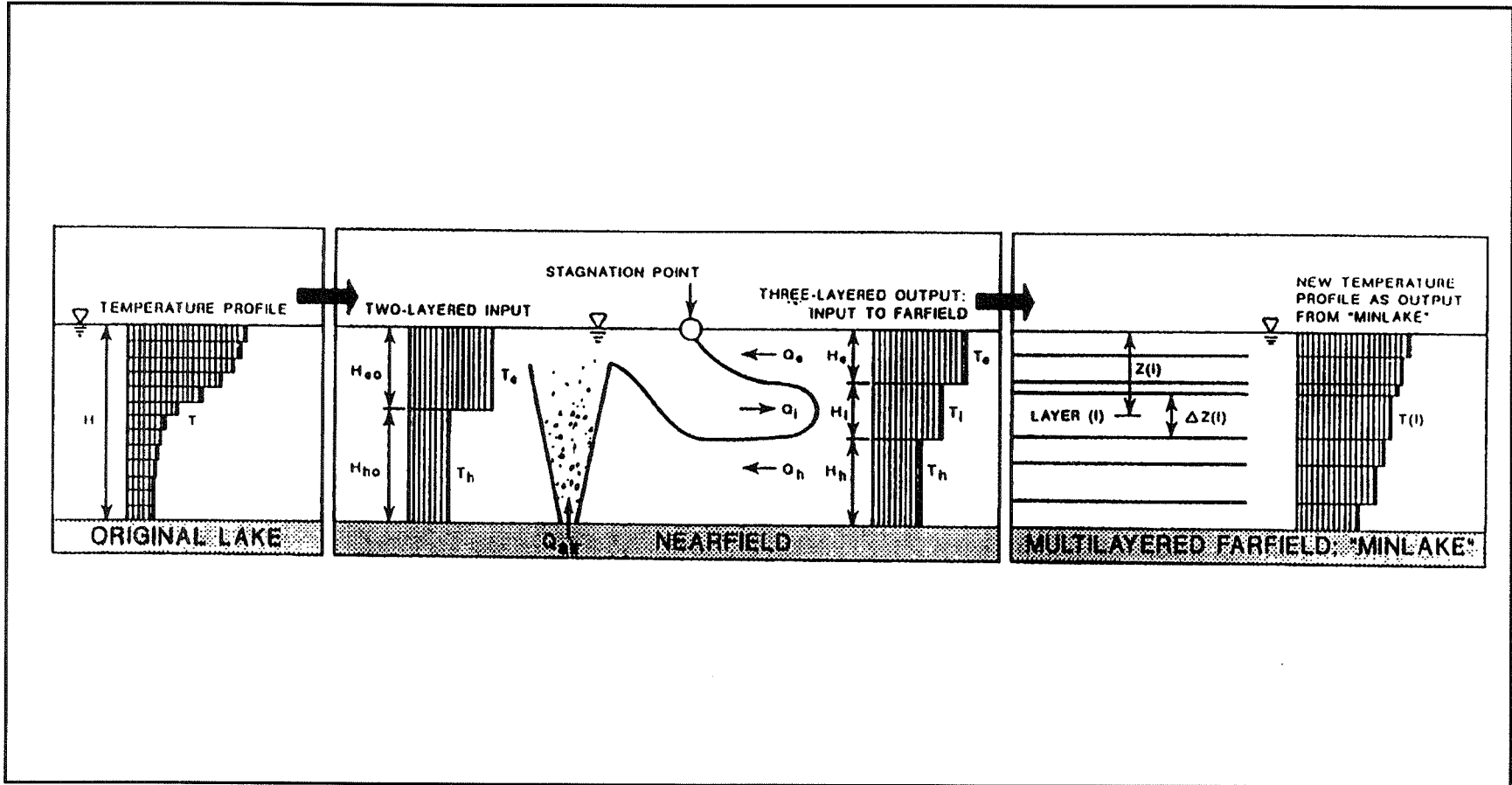


Figure 3. Schematic presentation of information flow

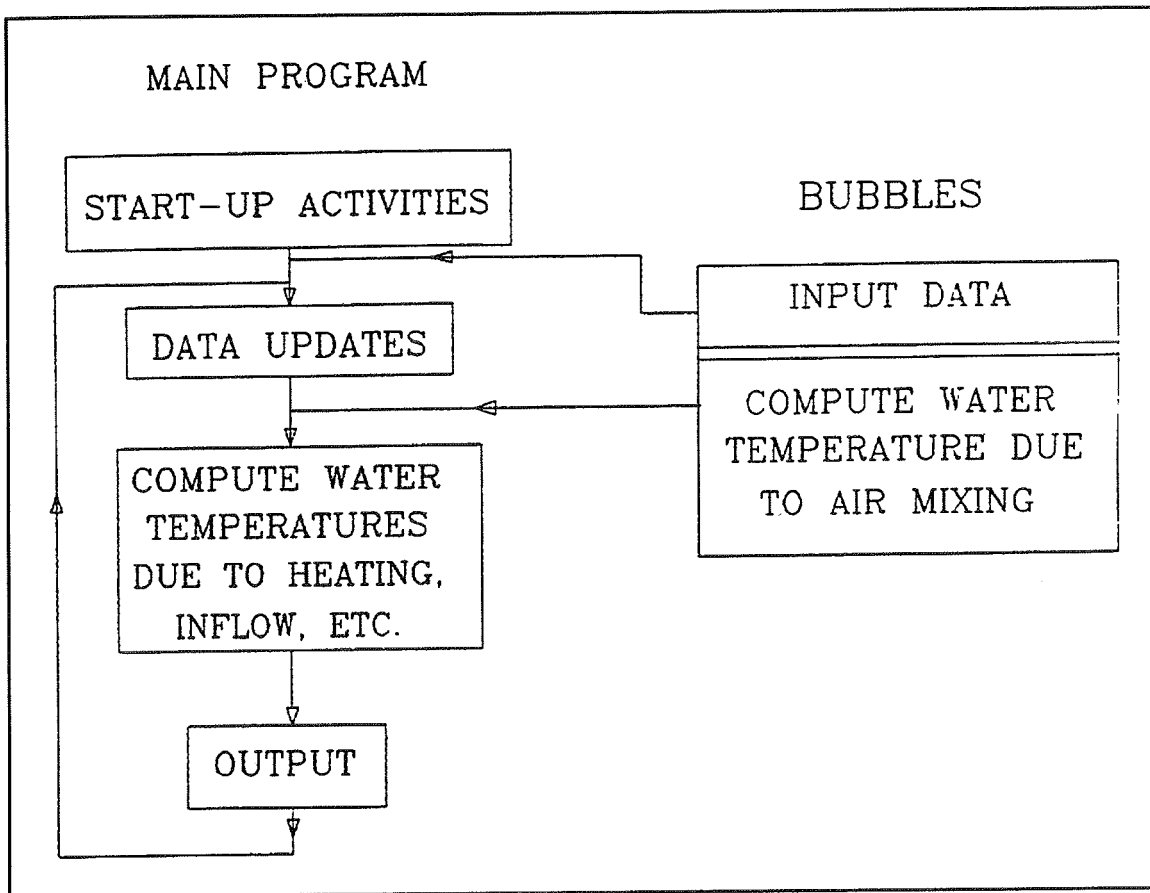


Figure 4. General flowchart

(Figure 7). A listing and definition of variables used in each subroutine are given in Appendix B.

The mixing routine is executed for each computational time step unless it conflicts with some criterion defined by the user. The air mixing routine will not be executed (or air will be shut off) if the temperature difference between the water surface and the diffuser depth drops under 1 °C (in TWOLAY).

Input Data Requirements

Since the subroutine BUBBLES is an addition to the main program, the user must provide all the data files required by the main program (Appendix C) plus the additional file of data describing the air mixing system. The data required to calculate the mixing by the air bubble column consists of the following information:

AIRIN - air flow rate at atmospheric condition, m³/sec

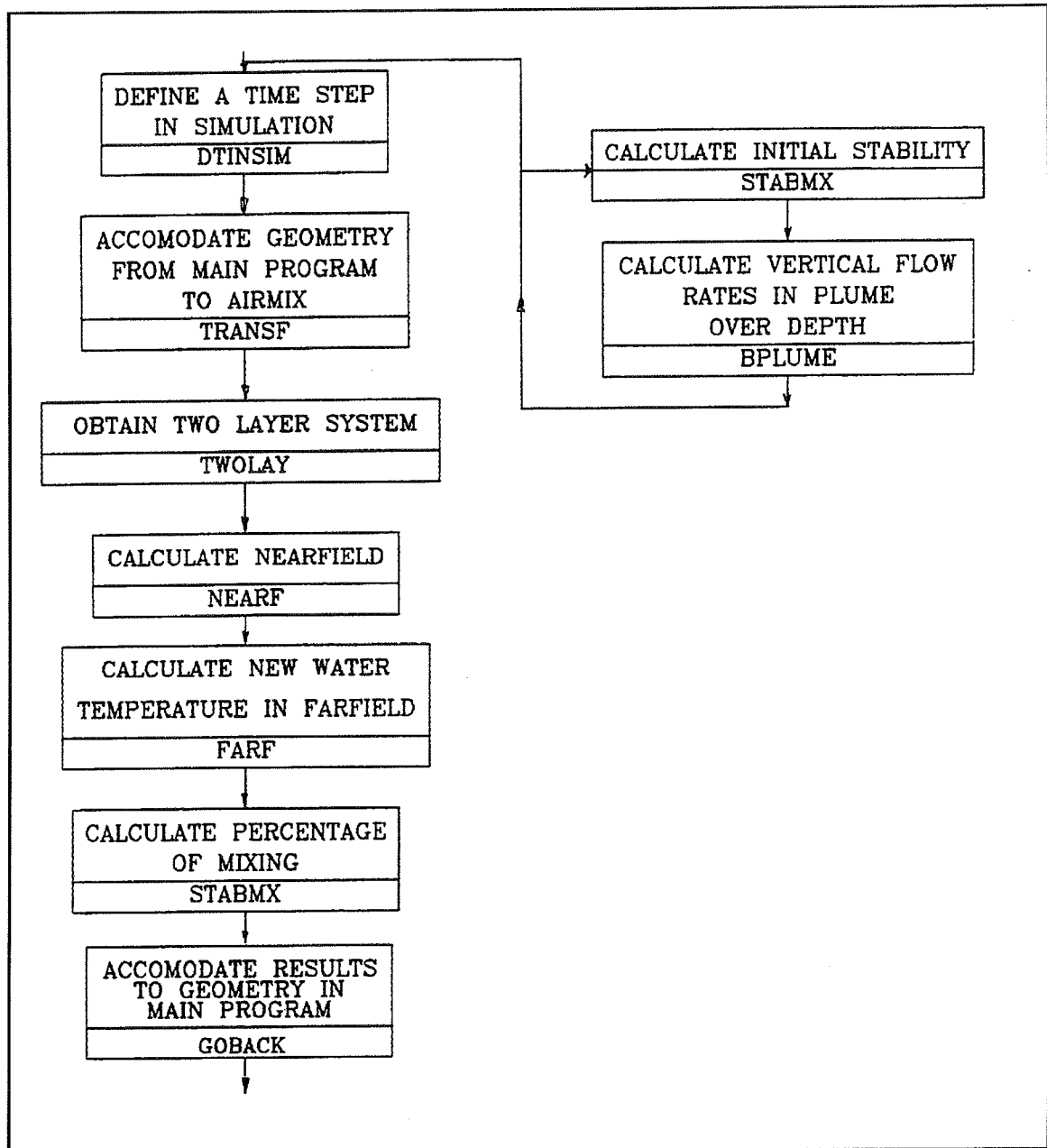


Figure 5. Flowchart for air mixing routine

HDIF - depth of diffuser, measured from the surface, m

ACARDS - number of following cards which define operation

ANDIFF - number of point diffusers

ASTART - Start day for air flow, JULIAN

ASTOP - Stop day for air flow, JULIAN

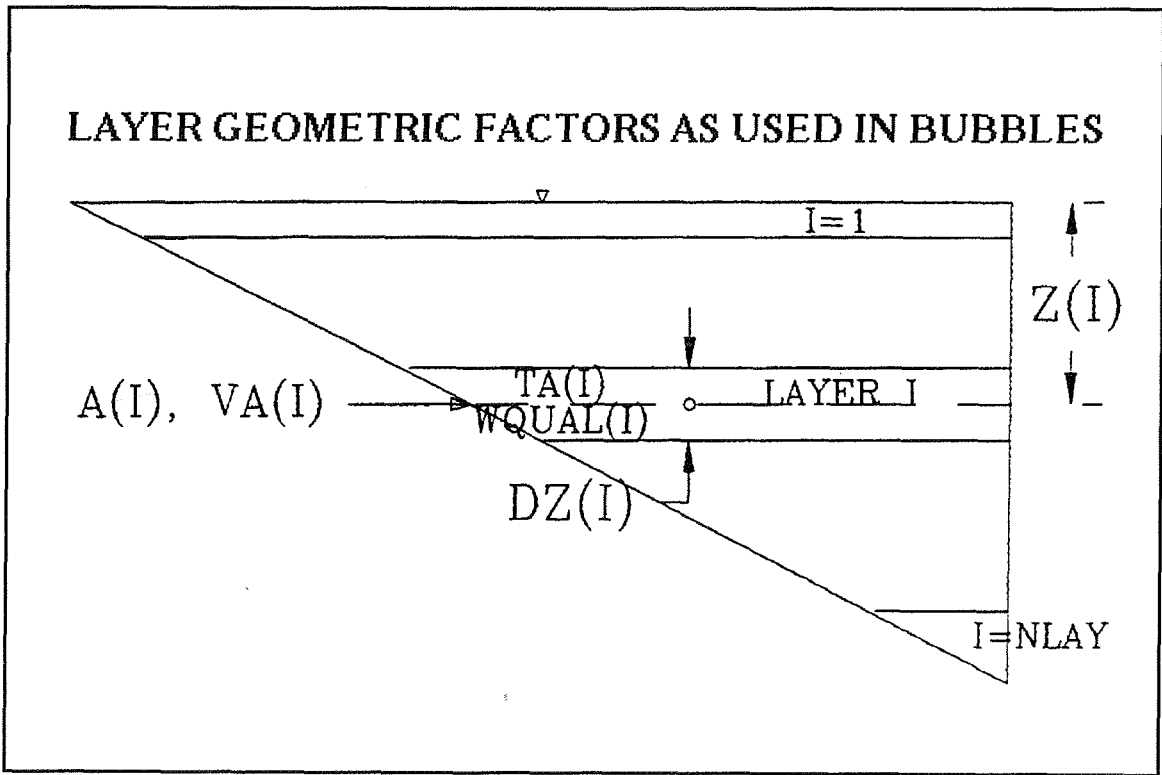


Figure 6. Notation used in air mixing routine

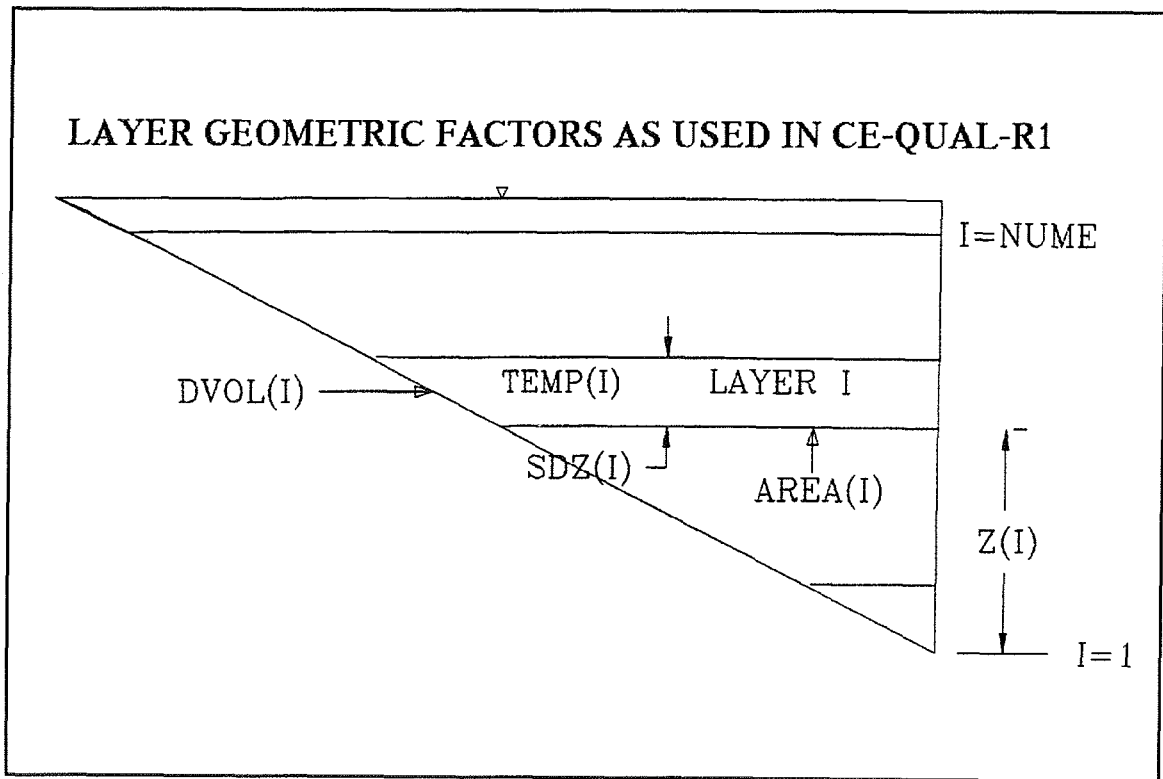


Figure 7. Notation used in CE-QUAL-R1

ADUR - Duration of air flow during day, hr

EPI - Epilimnion entrainment coeff

If more than one air bubble diffuser is used, it is assumed that they are positioned far enough from each other so that they do not interfere with each other. Therefore, the region affected by one diffuser is taken to be equal to the total area of the lake divided by the number of diffusers. Default is one diffuser.

The input data have to be written in free format in a file named AIRINP.DAT. Comment lines that include a title line were added for the convenience of the user. For the Lake Calhoun simulations, the file appeared as follows:

```
LAKE CALHOUN 1972          AIRINP.DAT
ANDIFF,          HDIFF,          ACARDS
1.0              19.0             1
Astart,          Astop,          ADUR,          AIRIN
218              243             24.0          .0590

COEFF - EPI ENTRAINMENT
0.30
```

The output file called AIROUT.DAT will contain the information about the input data as well as the number of time units elapsed with the air diffuser operating, the percentage of mixing achieved, and the interlayer flow Q_i , as shown in Appendix D.

Incorporation into CE-THERM-R1

CE-THERM-R1 (Environmental Laboratory 1982) is a numerical model that describes the vertical distribution of thermal energy in a reservoir over time. A definition sketch for the notation used in CE-THERM-R1 is shown in Figure 7. Sequence and timing of CE-THERM-R1 elements with subroutine BUBBLES is shown in Figure 8.

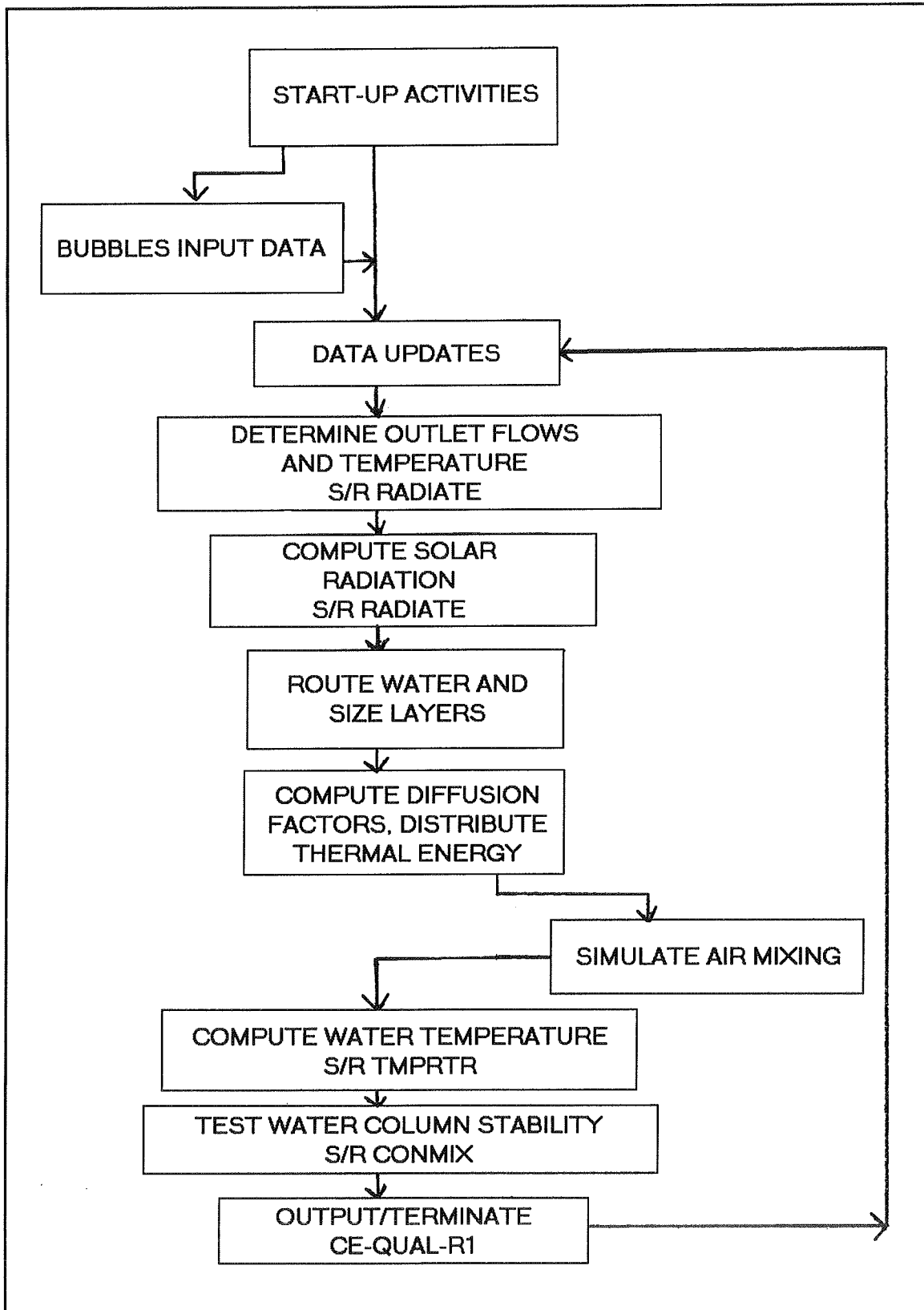


Figure 8. Sequence of CE-THERM elements and air mixing routine

4 Model Validation

Laboratory experiments (Zic, Stefan, and Ellis 1989) verified the basic assumptions of the mathematical model and generated the data to validate the model. The experiments were performed in a cylindrical basin 4.52 m in diameter and 1.1 m deep. The water temperatures were measured in a plane of the radial symmetry at four locations with eight thermistors at each location with accuracy of 0.1 °C. Typically, experiments ran for about 2 hr with a sampling interval of 15 sec. The analysis of the experimental data is presented by Zic, Stefan, and Ellis (1989) showing that the basic assumptions of the model are physically realistic. The results of the simulation of the experiments are shown here in Figures 9 to 14 and in Table 3 where H_t is a total depth. FD is a lake densimetric Froude number as formulated by Orlob (1983) as guidance for the applicability of the one-dimensional approximation to a lake

$$FD = \frac{L}{H} \frac{Q}{V} \sqrt{\frac{\rho_r \bar{H}}{g \Delta \rho}} \quad (29)$$

where

L = length of the lake

Q = average flow-through rate (here average Q_1)

H = average depth

$\Delta \rho$ = density difference over the depth \bar{H}

For $FD < 1/\pi$, one-dimensional models are applicable for a given situation (all the cases considered here). Constrained regression statistics is used as a measure of the goodness of fit between model and measurements. The regression is constrained through the origin to provide a direct regression of measurements to model results. The regression coefficient (r^2) is the ratio of the variance of the measurements explained by the regression to the total variance in the measurements.

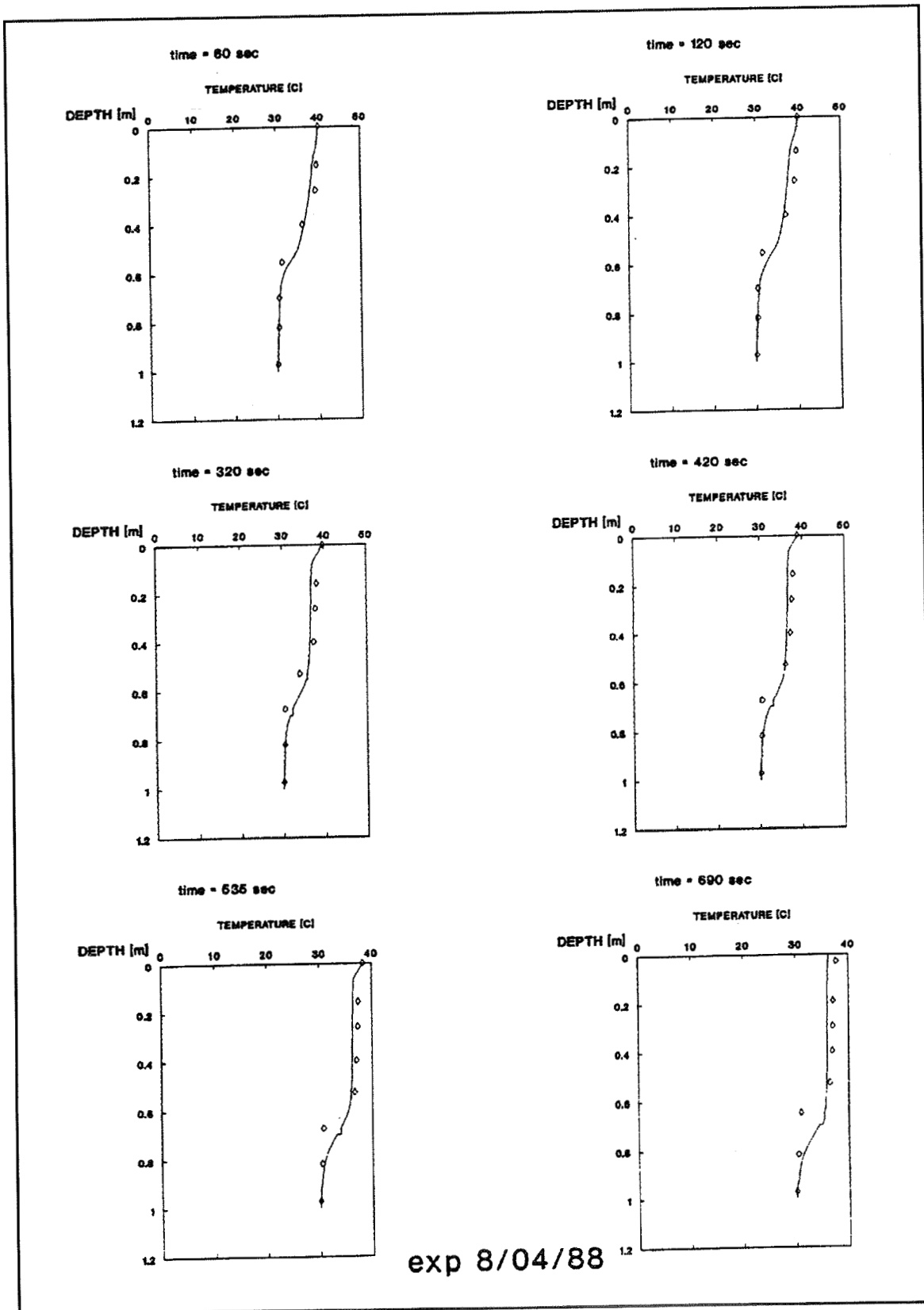


Figure 9. Simulation of destratification in laboratory experiment 8/04/88 (data from Zic, Stefan, and Ellis (1989))

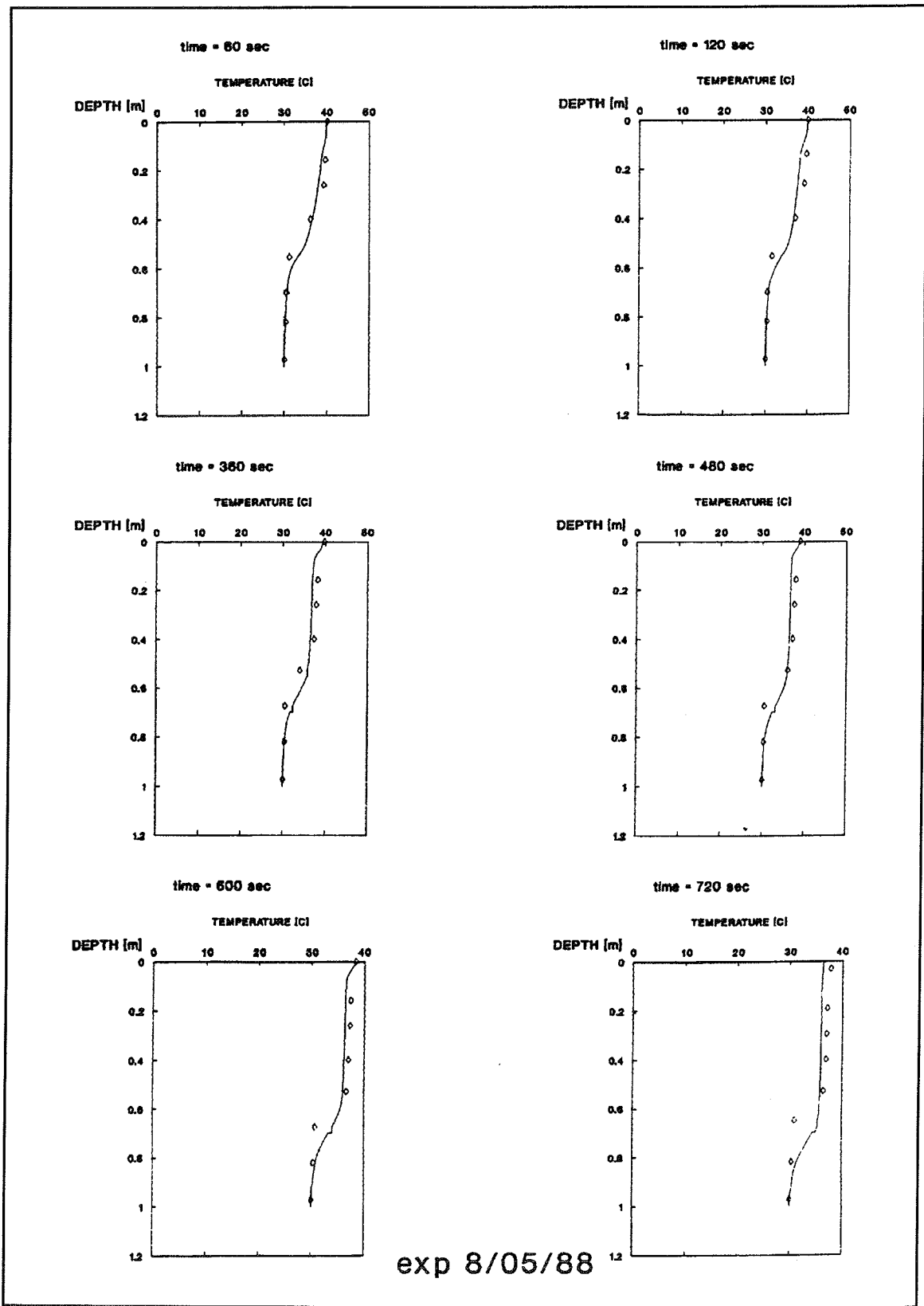


Figure 10. Simulation of destratification in laboratory experiment 8/05/88 (data from Zic, Stefan, and Ellis (1989))

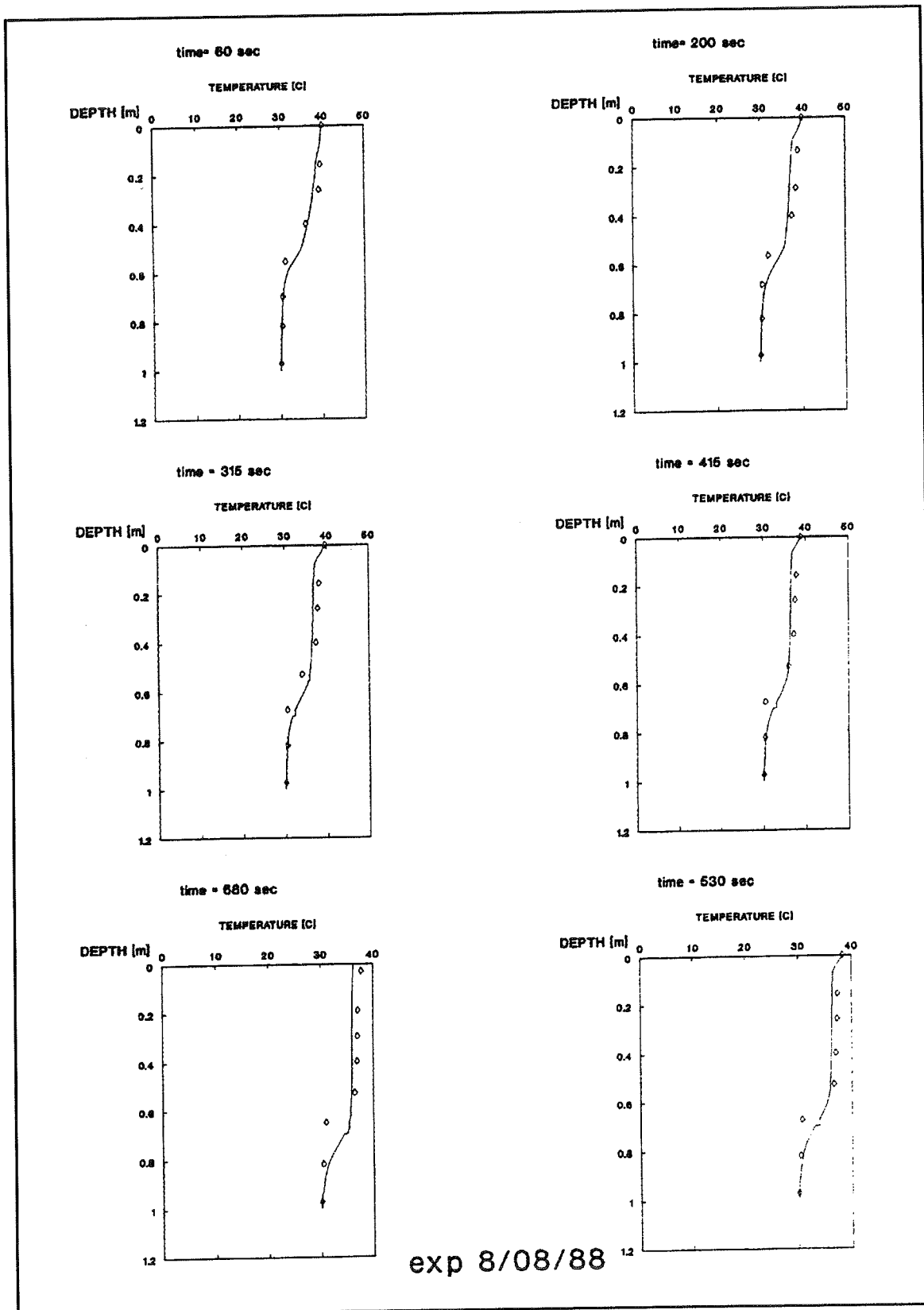


Figure 11. Simulation of destratification in laboratory experiment 8/08/88 (data from Zic, Stefan, and Ellis (1989))

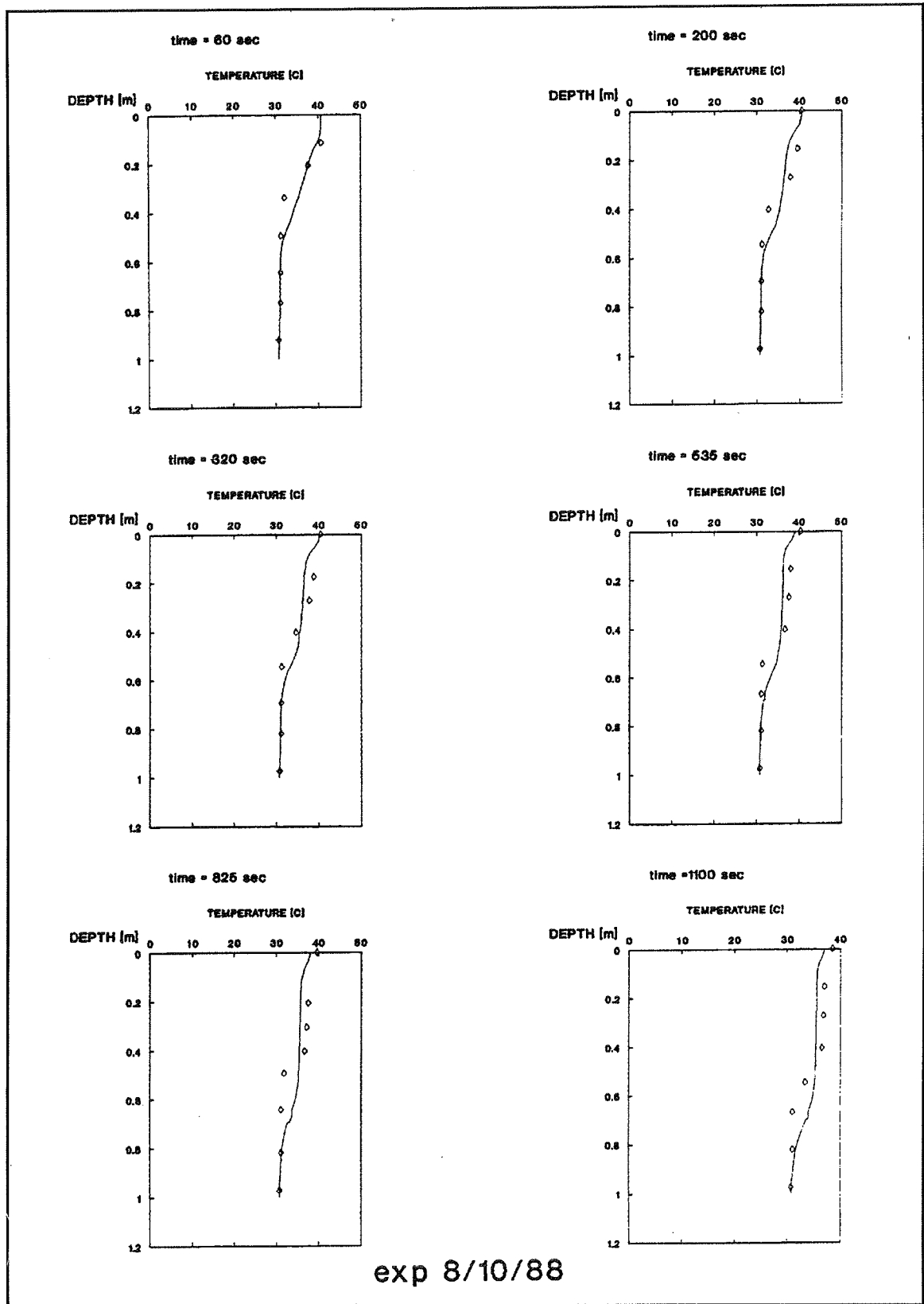


Figure 12. Simulation of destratification in laboratory experiment 8/10/88 (data from Zic, Stefan, and Ellis (1989))

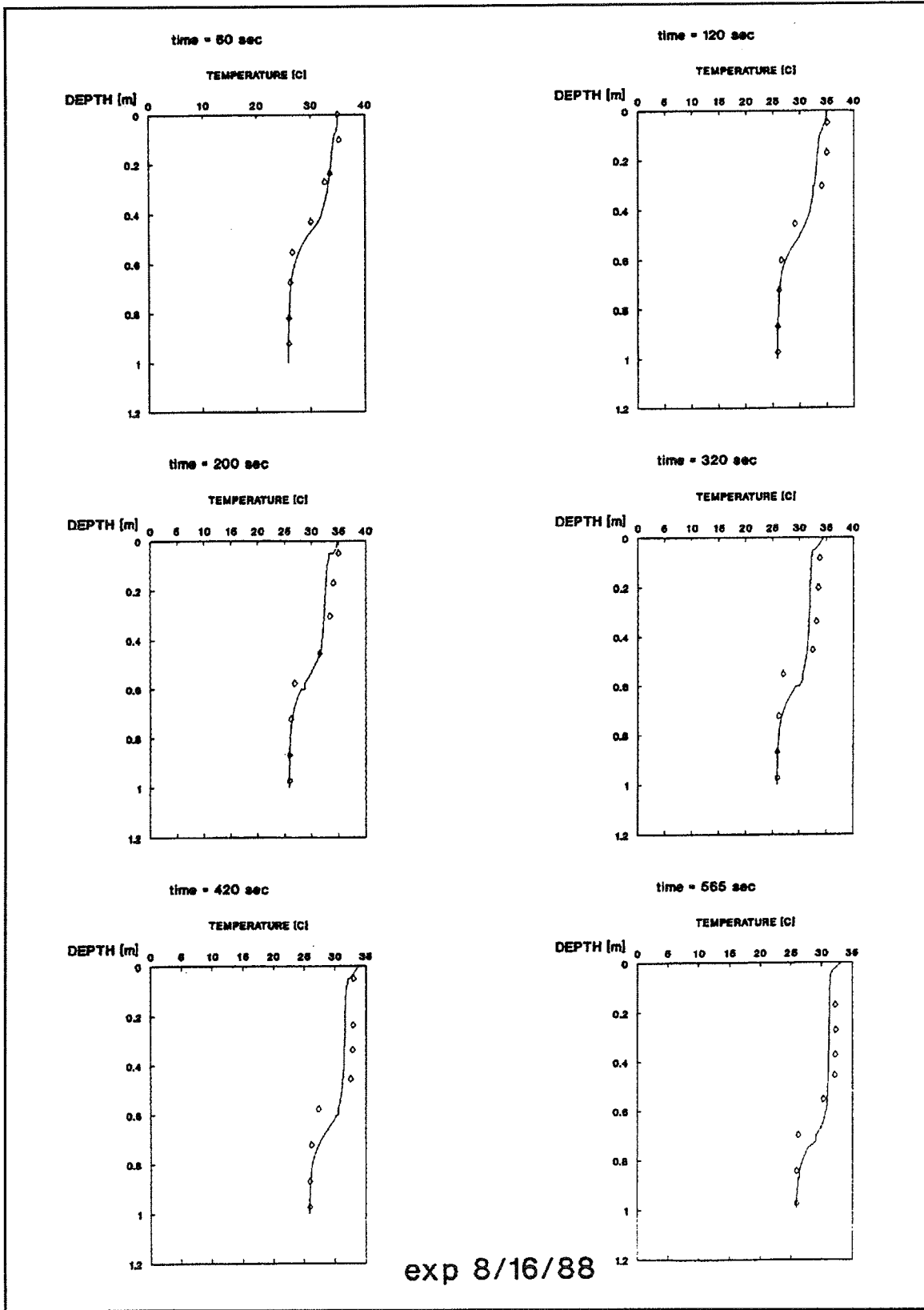


Figure 13. Simulation of destratification in laboratory experiment 8/16/88 (data from Zic, Stefan, and Ellis (1989))

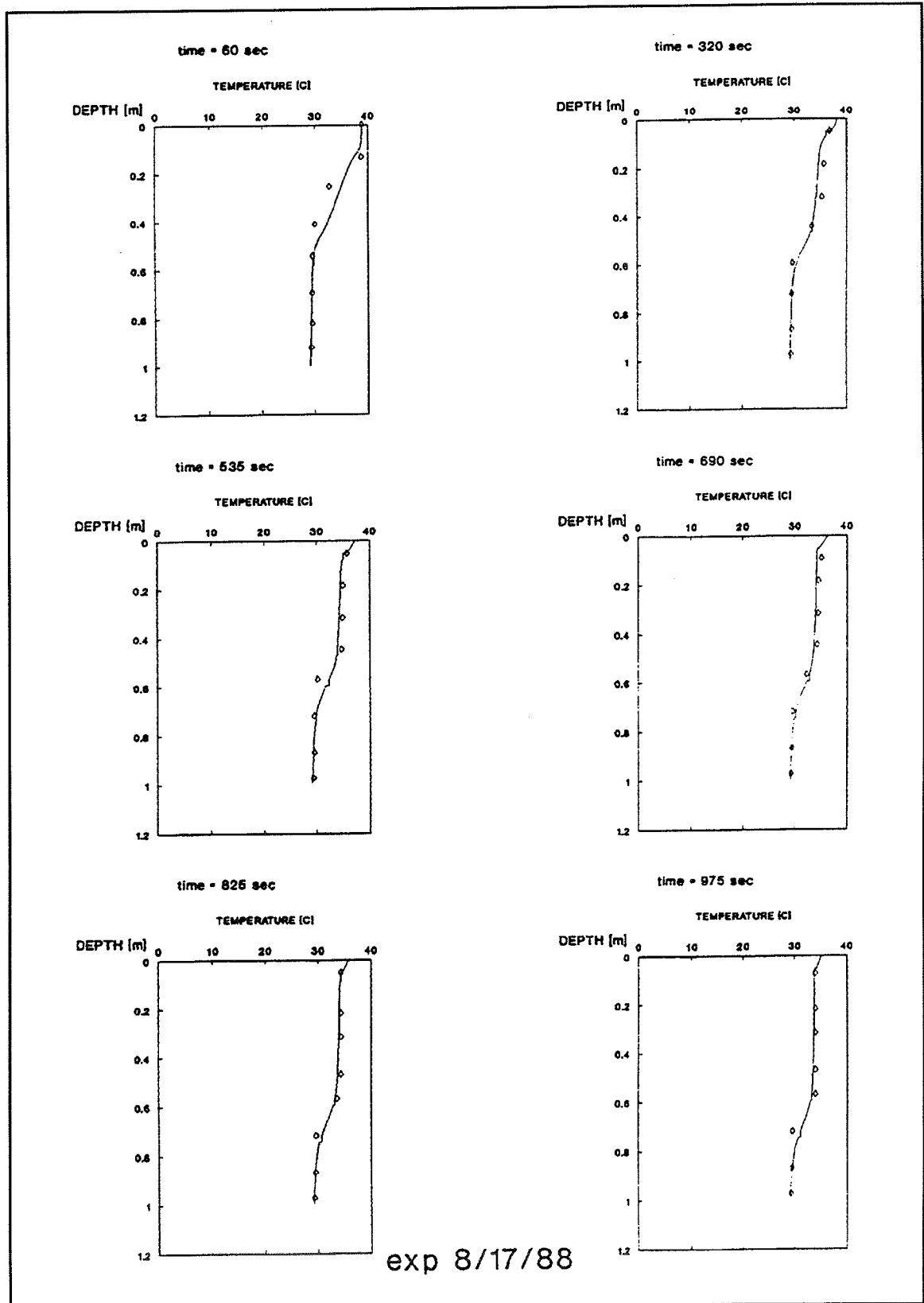


Figure 14. Simulation of destratification in laboratory experiment 8/17/88 (data from Zic, Stefan, and Ellis (1989))

Table 3
Simulation of the Experiments Performed in the Cylindrical Basin

Exp. Date	Q_{air} 1/sec	H , m	H_t , m	$\Delta T_{t=0}$ °C	$P\Delta$	FD	Simulations ($T_{meas} - T_{sim}/max$)		r^2
							°C	%	
8/10/88	0.133	0.81	1.0	9.8	0.147	0.02	2.7	5	0.9
8/4/88	0.3	0.81	1.0	5.1	0.029	0.03	1.4	5	0.94
8/8/88	0.353	0.81	1.0	10.2	0.070	0.02	3.1	10	0.95
8/5/88	0.458	0.81	1.0	5.0	0.016	0.02	0.9	3	0.97
8/17/88	0.155	0.83	1.02	9.6	0.117	0.03	2.6	9	0.94
8/16/88	0.392	0.83	1.02	9.0	0.045	0.04	2.6	10	0.91

The maximum temperature differences shown in Table 3 occur always at the position of the thermocline where a small error in the vertical position between the measured and simulated temperature profile results in a bigger error in the temperature. Based on r^2 , the simulation results give a good prediction of the destratification process.

The computer program was also applied to the field case, aeration of Lake Calhoun, Minneapolis, Minnesota (Shapiro and Pfannkuch 1973). The basic data for Lake Calhoun are as follows: mean depth = 10.0 m, maximum depth = 27.4 m, surface area = 1.71 km², volume = 17.1 × 10⁶m³. An estimated 0.0147 to 0.059 m³/sec = 0.005 to 0.021 m³min⁻¹ha⁻¹ = 0.067 to 0.27 ft³ min⁻¹acre⁻¹ of air were used. With an average inter-layer flow of 10 m³/sec FD = 0.002. Aeration of Lake Calhoun during the summer of 1972 lasted from August 3 to September 13. The aerator was a 30-m-long, 5-cm-diameter, perforated tube. Temperatures were measured with Yellow Springs Model 43T3 Telethermometer with accuracy 0.1 °C at one location in the far field, 200 m from the bubble plume. Meteorological data used in the simulations are from the nearby airport (about 5 miles away). A bathymetric map was provided by Minnesota Department of Natural Resources with isohyets 10 ft apart, as shown in Figure 15. The data file for input to the model is shown in Appendix C. The results of the calibration runs for summer 1971 for CE-THERM-R1 are shown in Figure 16. Results of the simulation of the destratification in 1972 are shown in Figure 17.

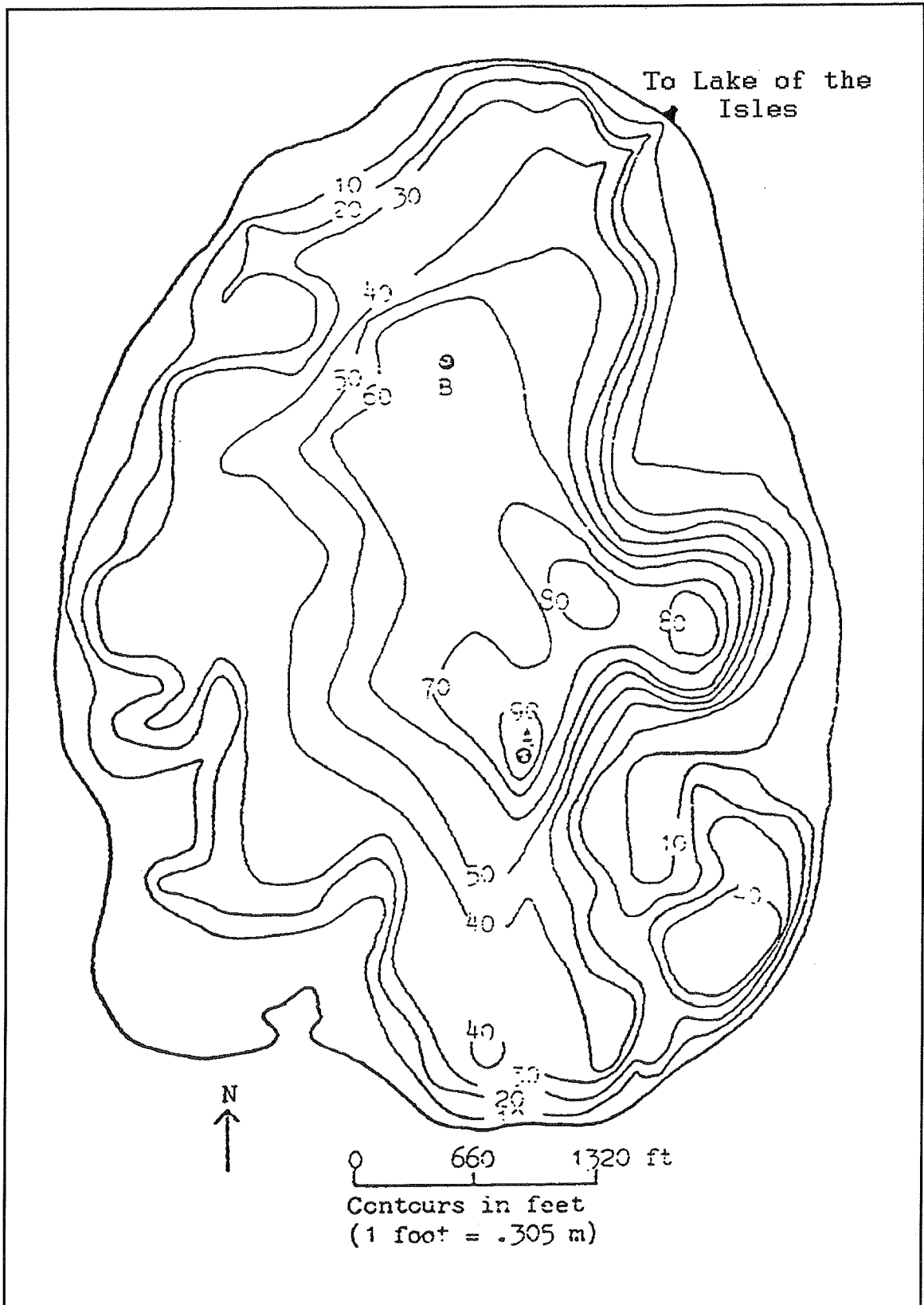


Figure 15. Bathymetric map of Lake Calhoun

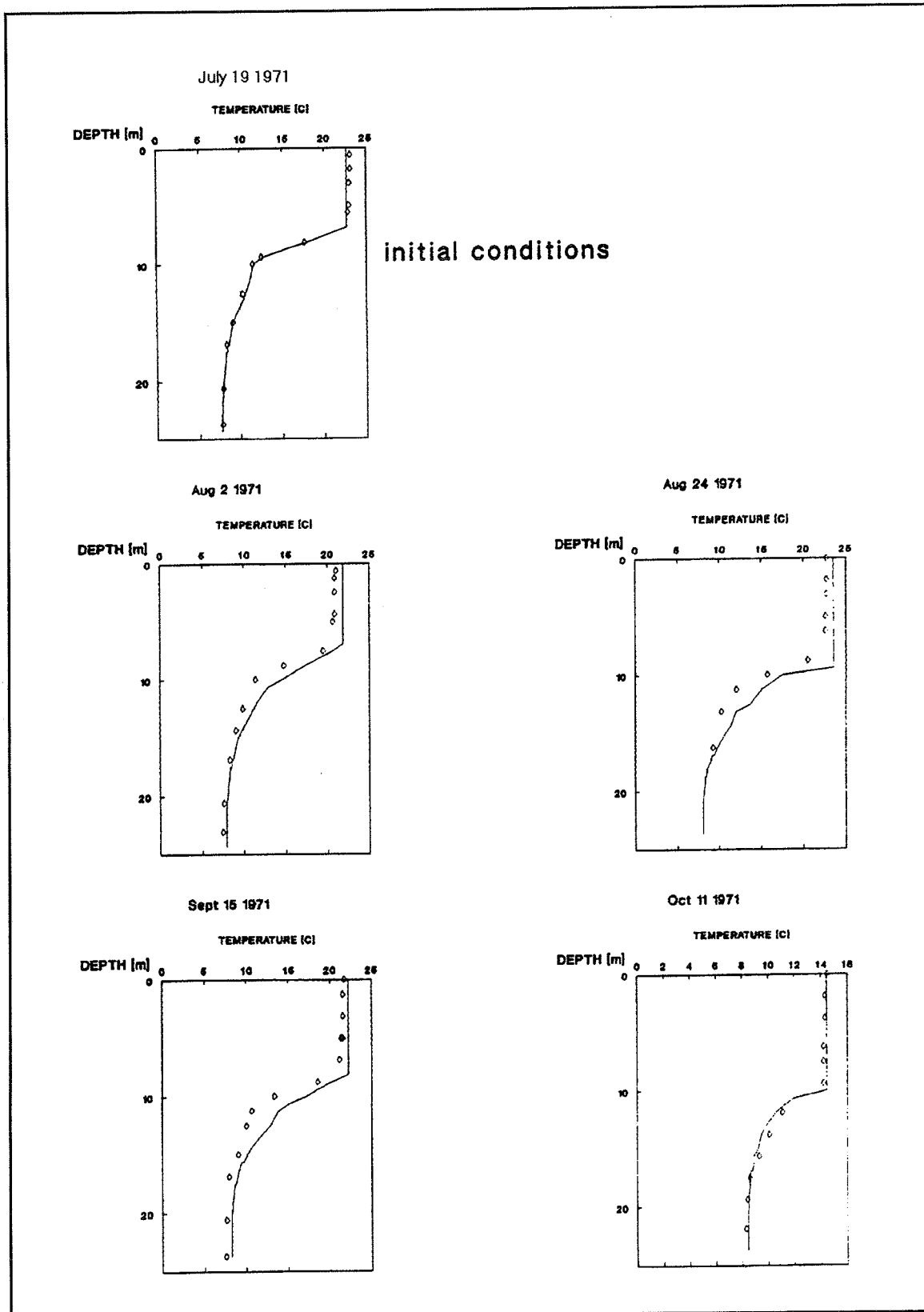
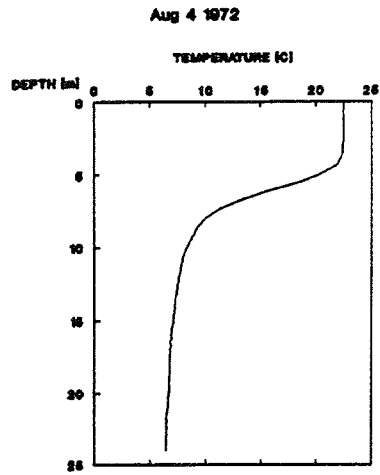


Figure 16. Calibration results for CE-QUAL-R1 (Lake Calhoun) (data from Shapiro and Pfannkuch (1973))

main program : CE-QUAL-R1



initial conditions

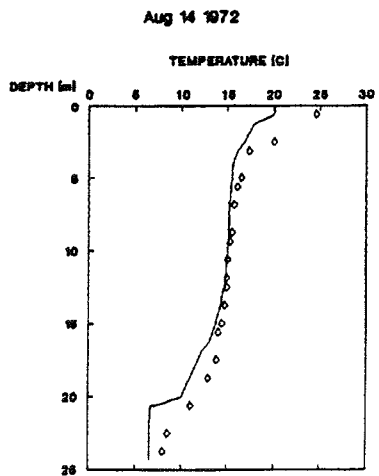
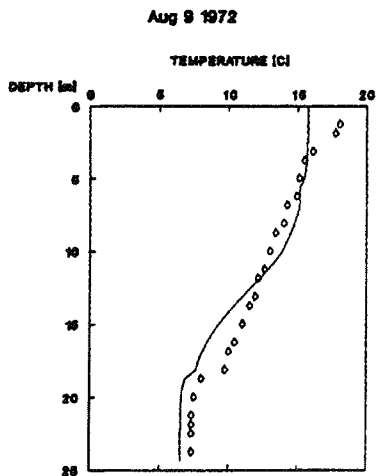
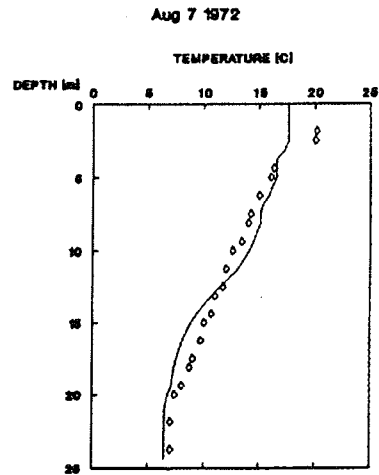
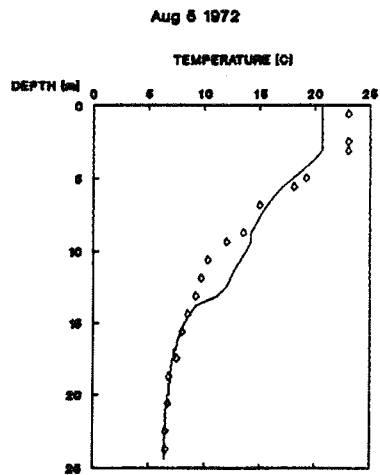


Figure 17. Simulation of destratification of Lake Calhoun (data from Shapiro and Pfannkuch (1973)) (Continued)

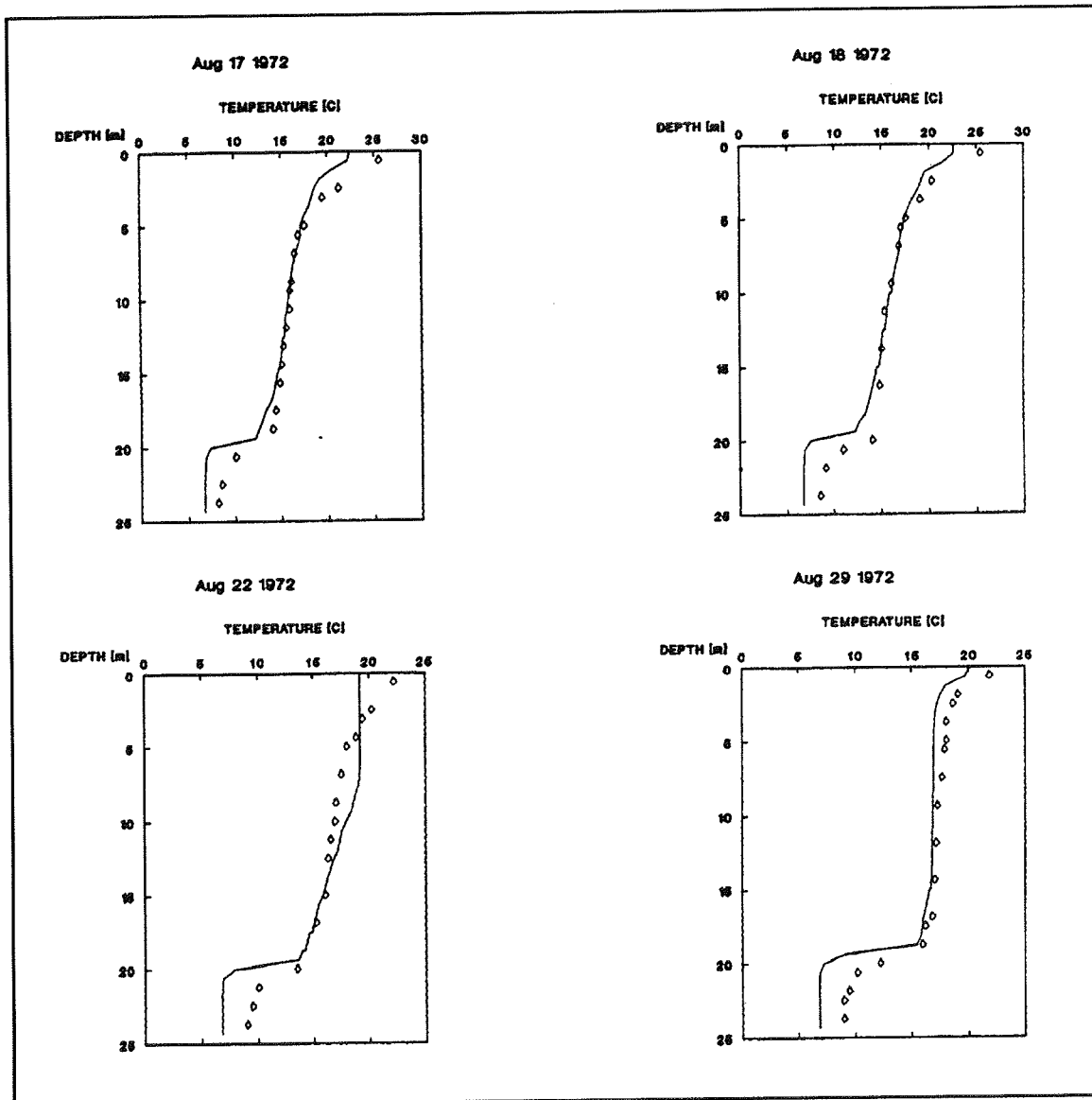


Figure 17. (Concluded)

5 Summary

Destratification is a means of improving the quality (dissolved oxygen content) of a reservoir or lake by mixing the water body, thereby preventing thermal and chemical stratification. If the thermal stratification can be minimized or eliminated, wind mixing and artificially induced circulation can transport high quality water throughout the water column. A detailed account of the limnological effects of destratification is given by Pastorok, Lorenzen, and Ginn (1982).

Generally, there are two methods for artificially mixing a reservoir or lake: hydraulic mixers that pump water or pneumatic diffusers that move water with a rising bubble plume. Both techniques have been used for lake destratification or to locally mix a portion of a lake. For reservoir destratification, a pneumatic system is probably more cost-effective (costs of high volume water pumps are usually much greater than air compressors).

There is little design or operational guidance for long-term (seasonal) operation of a destratification system. Thus, a numerical description of pneumatic destratification was developed and incorporated into a dynamic one-dimensional reservoir model. The model CE-THERM-R1 is capable of simulating the thermal and heat budgets of a reservoir. Incorporating the numerical model of destratification BUBBLES adds the capability of predicting the effects of a destratification system and provides information about system operation.

The BUBBLES algorithm was based on the work of Goossens (1979) and validated with laboratory observations (Zic, Stefan, and Ellis 1989) and field observation from Lake Calhoun, Minnesota (Shapiro and Pfannkuch 1973)). In general, the model satisfactorily predicts the performance of the destratification system. However, a caution must be issued regarding applications to reservoirs: in most instances, the morphometry of a reservoir is significantly different from a natural lake or the laboratory facility. The morphological differences between a lake and a reservoir may present different destratification characteristics, especially in the development of the interflow in the far field. Lake Calhoun is a bowl-shaped lake, while most reservoirs are very long and narrow.

The type of diffuser described by the mathematics of the BUBBLES algorithm is a point source of bubbles. This type of diffuser produces a radial circulation cell around the diffuser. An explicit assumption in the model is that multiple diffusers are hydrodynamically separated and do not interact or interfere with each other. A line diffuser produces linear circulation cells on each side of the diffuser, but may be approximated by a point source depending upon the length of the diffuser relative to the water body. Thus, judgment must be exercised when analyzing results if a linear diffuser is proposed.

The model is recommended for evaluation of destratification systems, but care must be exercised in analyzing the results from reservoirs. Few reservoirs are bowl-shaped; however, reservoirs often exhibit a bowl-shaped morphology at some location in which a diffuser may be placed and good results obtained. Continued model development is recommended to address the limitations associated with the shape of the water body. As discussed in the previous paragraph, currently the type of diffuser cannot be defined (point-source or linear). Additional analysis and characterization of line diffusers is recommended.

References

- Asaeda, T., and Imberger, J. (1988). "Structures of bubble plumes in stratified environments," Environmental Dynamics Report ED-88-250, Center for Water Research, University of Western Australia, Nedlands, WA.
- Cederwall, K., and Ditmars, J. D. (1970). "Analysis of air-bubble plumes," Report No. KH-R-24, W. M. Keck Laboratory of Hydraulics and Water Resources, California Institute of Technology, Pasadena, CA.
- Davis, J. M. (1980). "Destratification of reservoir—a design approach for perforated-pipe compressed-air systems," Water Services, 497-504.
- Ditmars, J. D. (1970). "Mixing of density-stratified impoundments with buoyant jets," Report No. KH-R-22, W. M. Keck Laboratory, California Institute of Technology, Pasadena, CA.
- Dortch, M. S. (1979). "Artificial destratification of reservoirs," Technical Report E-79, U.S. Army Engineer Waterways Experiment Station, Vicksburg, MS.
- Environmental Laboratory (1982). "CE-QUAL-R1: A numerical one-dimensional model of reservoir water quality - user's manual," Instruction Report E-82-1, U.S. Army Engineer Waterways Experiment Station, Vicksburg, MS.
- Ford, D. E., and Stefan, H. G. (1980). "Thermal predictions using integral energy model," *Jour. Hydraulics Division, ASCE*, 106 (HY1), 39-35.
- Goossens, L. (1979). *Reservoir destratification with bubble column*. Delft University Press.
- Graham, D. S. (1978). "Experimental results of destratification by buoyant plumes." *Proc. of 2nd Annual Waste Heat Conf.* University of Miami, Miami Beach, FL, 1028-1046.

- Hossain, N. A., and Narang, B. S. (1983). "Simplified analysis of air bubble plumes in moderately stratified environments," *Jour. Heat Transfer*, ASME 106, 543-551.
- Imberger, J., and Patterson, J. C. (1981). "A dynamic reservoir simulation model, DYRESM: 5." *Transport models for inland and coastal waters*. H. B. Fischer, ed., Academic Press, New York, 310-361.
- Ito, T. (1972). "Mixing method of stratified water layer in reservoir." *Int. Symp on Stratified Flows, Novosibirsk*.
- Johnson, T. R., Ellis, C., and Stefan, H. G. (1989). "Negatively buoyant flow in diverging channel. IV: Entrainment and dilution," *Jour. Hydraulic Division*, ASCE 115 (4), 437-456.
- Knoppert, P. L., Rook, J. J., Hofker, T., and Oskam, G. (1970). "Destratification experiments of Rotterdam," *Jour*, AWWA 62, 448-454.
- Kobus, H. E. (1968). "Analysis of the flow induced by air-bubble systems." *Proceedings of the 11th International Conference in Coastal Engineering*. London, 1016-1031.
- _____. (1973). *Bemessungsgrundlagen und Anwendungen für Luftschleier im Wasserbau*, Erich Schmidt Verlag.
- Kranenburg, C. (1979). "Destratification of lakes using bubble columns," ASCE, *Jour. of Hydr. Div.* 105, HY4, 333-349.
- McDougall, J. T. (1978). "Bubble plumes in stratified environments," *J. Fluid Mechanics* 85(4), 655-72.
- Milgram, J. H. (1983). "Mean flow in round bubble plumes," *Jour. of Fluid Mechanics* 133, 345-376.
- Orlob, G. T., ed. (1983). *Mathematical modeling of water quality in streams, lakes and reservoirs*. Wiley & Sons, New York.
- Pastorok, R. A., Lorenzen, M. W., and Ginn, T. C. (1982). "Environmental aspects of artificial aeration and oxygenation of reservoirs: A review of theory, techniques, and experiences," Technical Report E-82-3, U.S. Army Engineer Waterways Experiment Station, Vicksburg, MS.
- Patterson, J. C., and Imberger, J. (1989). "Simulation of bubble plume destratification systems in reservoirs," *Aquatic Sciences* 51(1), 3-18.
- Poon, Y. C. (1985). "Modeling of round bubble plumes," M.S. thesis, University of Calgary, Alberta, Canada.

- Price, R. E. (1988). "Applications of mechanical pumps and mixers to improve water quality," Water Operations Technical Support Bulletin E-88-3, 6-9.
- Punnet, R. E. (1991). "Design and operation of axial flow pumps for reservoir destratification," Instruction Report W-91-1, U.S. Army Engineer Waterways Experiment Station, Vicksburg, MS.
- Riley, M., and Stefan, H. G. (1987). "Dynamic lake water quality model MINLAKE," Project Report No. 263, St. Anthony Falls Hydraulic Laboratory, University of Minnesota, Minneapolis, MN.
- _____. (1988). "MINLAKE: A dynamic lake water quality simulation model," *Ecological Modeling* 43, 155-182.
- Rowe, R. D., Poon, J. Y. C., and Laureshen, C. J. (1989). "A simple method for predicting bubble plume properties," XXIII IAHR Congress, Ottawa, Canada, D-23-D-30.
- Shapiro, J., and Pfannkuch, H. O. (1973). "The Minneapolis chain of lakes - A study of urban drainage and its effects, 1971-1973," Interim Report No. 9, Limnology Research Center, University of Minnesota, Minneapolis, MN.
- Stefan, H. G., and Ford, D. E. (1975). "Temperature dynamics in dimictic lakes," ASCE, *Jour. of Hydr. Div.* 101 (HYI), 977-113.
- Tekeli, S., and Maxwell, W. H. C. (1978). "Behavior of air bubble screens," Technical Report UILU-ENG-78-2019, University of Illinois at Urbana, Champaign, IL.
- Tsang, G. (1984). "Modelling criteria for bubble plumes - a theoretical approach," *Can. Jour. Civ. Eng.* 11, 293-298.
- Zic, K. (1990). "Analysis and simulation of mixing of stratified lakes or reservoirs by air bubble plumes," Ph.D. diss., University of Minnesota, Minneapolis, MN.
- Zic, K., and Stefan, H. G. (1988). "Lake aerator effect on temperature stratification analyzed by MINLAKE model," *Lake and Reservoir Management*, 4(2), NALMS, 85-90.
- _____. (1990). "Analysis and simulation of mixing of stratified lakes or reservoirs by air bubble plumes," Proj. Report No. 305, St. Anthony Falls Hydraulic laboratory, University of Minnesota, Minneapolis, MN.
- Zic, K., Stefan, H. G., and Ellis, C. (1989). "Laboratory study of bubble plume destratification," *Jour. Hydraulic Research*, IAHR.

Appendix A

Bubble Plume Model by Poon (1985)¹

Assuming Gaussian profiles for the vertical plume velocity, the density deficit in the bubble plume and isothermal expansion for air bubbles, Poon (1985) found that the equations of conservation of mass, conservation of momentum, and conservation of buoyancy in the isothermal environment can be respectively written as:

$$2 \alpha U(z) b(z) = \frac{d}{dz} U(z) b^2(z) \left\{ 1 - \frac{\lambda^2 \Delta \rho(z)}{[1 + \lambda^2][\rho_a(z) - \rho_g(z)]} \right\} \quad (\text{A1})$$

$$g \lambda^2 \Delta \rho(z) b^2(z) = \frac{d}{dz} \gamma b^2(z) \left\{ U^2(z) \left[\frac{\rho_a(z)}{2} - \frac{\lambda^2 \Delta \rho(z)}{1 + 2\lambda^2} \right] + \right. \quad (\text{A2})$$

$$\left. \frac{\lambda^2 u b \rho_g(z) \Delta \rho(z)}{\rho_a(z) - \rho_g(z)} \left[\frac{2 U(z)}{1 + \lambda^2} + \Delta u_b \right] \right\}$$

$$\frac{\pi \lambda^2 \Delta \rho(z) b^2(z) g U(z)}{[1 + \lambda^2][\rho_a(z) - \rho_g(z)]} = \frac{Q_{air} P_a U(z)}{[H_B - z][1 + \lambda^2][\rho_a(z) - \rho_g(z)]} \quad (\text{A3})$$

where

z = height measured upward from the diffuser

U = centerline velocity

b = plume radius

ρ_a = ambient density

¹ References cited in this appendix are located at the end of the main text.

- $\Delta\rho$ = density deficiency at the plume centerline
 λ = ratio of gas containing radius to plume radius (called also a dispersion coefficient)
 α = entrainment coefficient
 γ = momentum amplification factor
 H_B = pressure head at the level of gas release, $H_B = H_T + H$
 H_T = atmospheric pressure head (= 10.2 m)
 H = submergence depth of diffuser
 Δu_b = bubble relative (slip) velocity = 0.25 (m/sec)
 p_a = atmospheric pressure

The values for the coefficients α , λ , and γ are given by Poon (1985):

$$\alpha(B_u) = 0.136 \left[\frac{B_u}{54.2 + B_u} \right]^{0.5} \quad (\text{A4})$$

$$\gamma(B_u) = 1.0 + \frac{16.2}{B_u^{1.30}}$$

$$\lambda(B_u) = 1.2 \left[\frac{B_u}{71 + B_u} \right]$$

where $B_u = \{\rho_r / (\sigma(Q^4 \text{air} g^3)^{0.2})\}^{0.5}$ is called Weber number for the plume, σ = surface tension. The initial conditions are given at the height of the zone of flow establishment z_e , initial momentum flux, and initial center-line plume density defect, respectively, as (Milgram 1983)

$$z_e = \min \left\{ \begin{array}{l} 5 D \\ 10 u_o \left(\frac{D}{g} \right)^{1/2} \\ \left[\frac{\rho_g(0)}{\rho_w} \right]^{3/4} \end{array} \right\} \quad (\text{A5})$$

$$M(z_e) = q_T \rho_g(H) u_o + \frac{2 q(0.5 z_e)}{u_o} [\rho_w - \rho_g(0.5 z_e)] g z_e \quad (\text{A6})$$

$$S(z_e) = 0.5 \rho_w \quad (\text{A7})$$

Equations A1 to A7 were solved using the Newton-Raphson method (Poon 1985) to obtain the water flow rate in the bubble plume for a given hypolimnetic thickness h_{hy} .

Appendix B

Variables Used in Program

BUBBLES

TA	TEMPERATURE OF I-TH LAYER	(°C)
ZA	DEPTH OF I-TH LAYER	(m)
DZ	THICKNESS OF I-TH LAYER	(m)
A	CROSS SECTIONAL AREA OF I-TH LAYER	(m ²)
VA	VOLUME OF I-TH LAYER	(m ³)
NLAY	NUMBER OF LAYERS IN A GIVEN SEQUENCE	
HTOT	TOTAL DEPTH	(m)
QEO	FLOW RATE IN EPILIMNION AT STAGNATION POINT	(m ³ /s)
QHO	FLOW RATE IN HYPOLIMNION AT STAGNATION POINT	(m ³ /s)
HEP	THICKNESS OF EPILIMNION AT STAGNATION POINT	(m)
HIN	THICKNESS OF INTERLAYER AT STAGNATION POINT	(m)
TEP	TEMPERATURE OF UPPER LAYER IN TWO LAYER SYSTEM	(°C)
THY	TEMPERATURE OF LOWER LAYER IN TWO LAYER SYSTEM	(°C)
HEP0	THICKNESS OF UPPER LAYER IN TWO LAYER SYSTEM	(m)
HHY0	THICKNESS OF LOWER LAYER IN TWO LAYER SYSTEM	(m)
IA	INDEX OF THE LOWER BOUNDARY OF INTERLAYER	
IB	INDEX OF THE UPPER BOUNDARY OF INTERLAYER	
IDIF	INDEX OF SUBMERGENCE DEPTH OF DIFFUSER	
DTSIM	TIME STEP IN A GIVEN SEQUENCE	(sec)
QAIR	VOLUMETRIC AIR FLOW RATE AT ATMOSPHERIC CONDITIONS	(m ³ /s)
HDIFF	SUBMERGENCE DEPTH OF DIFFUSER	(m)
HDIFF0	INITIAL THICKNESS AFFECTED BY ENTRAINMENT	(m)
ANDIFF	NUMBER OF POINT DIFFUSERS	
NDAYC	NUMBER OF TIME UNITS ELAPSED	
IDEPN	CONTROL INDEX	
STAB0	INITIAL STABILITY IN THE RESERVOIR	(J)
TELAP	TIME ELAPSED	(sec)
DELZ	LAYER THICKNESS IN WESTEX	(feet)
HD	DISTANCE BETWEEN DIFFUSER AND BOTTOM OF RESERVOIR	(m)
H0	INITIAL DISTANCE BETWEEN THERMOCLINE AND DIFFUSER	(m)
AAVE	AVERAGE CROSS SECTION AREA BELOW DIFFUSER	(m ²)

TIME0	TIME WHEN THERMOCLINE REACHES DIFFUSER'S DEPTH	(sec)
ZP	DEPTH AT WHICH FLOW RATE IN BUBBLE PLUME IS CALCULATED	(m)
QP	WATER FLOW RATE AT DEPTH ZP	(m ³ /s)
ICMAX	NUMBER OF ELEMENTS IN ZP AND QP ARRAYS	
DTSIM	TIME STEP IN A GIVEN SEQUENCE	(sec)
NSL	PARAMETER DEFINING THE SIZE OF ARRAYS (CORRESPONDS TO MAIN PROGRAM)	

subroutine: **DTINSIM**

DTSIM	TIME STEP IN A GIVEN SEQUENCE	(sec)
-------	-------------------------------	-------

subroutine: **TURNAIR**

QAIR	AIR FLOW RATE AT ATMOSPHERIC CONDITIONS	(m ³ /sec)
PDNUM	NUMBER OF POINT DIFFUSERS	
HIDIFF	SUMBERGENCE DEPTH OF DIFFUSER	(m)

subroutine: **STABMX**

VIRHO	MASS OF I-TH LAYER	(kg)
MIXING	MIXING ACHIEVED AT GIVEN TIME	(%)
QINTER	FLOW RATE IN INTERLAYER	(m ³ /s)
ZGSTR	CENTER OF MASS FOR STRATIFIED LAKE	(m)
ZAZRHO	SUMMATION TO OBTAIN ZGSTR.	
ZG	CENTER OF MASS FOR WELL MIXED LAKE	(m)
ZAZ	SUMMATION TO OBTAIN ZG	
VOLL	TOTAL VOLUME ABOVE DIFFUSER	(m ³)
STABT	STABILITY PARAMETER AT GIVEN TIME	(J)
VRHO	TOTAL MASS ABOVE DIFFUSER	(kg)
IDIF	INDEX OF SUBMERGENCE DEPTH OF DIFFUSER	

subroutine: **TWOLAY**

IFOUR	INDEX OF MINIMUM THICKNESS OF UPPER LAYER IN TWO LAYER SYSTEM ALLOWED	
ZIMAX	INDEX DEFINING POSITION OF THERMOCLINE ((ITHBOT+ITHUP)/2)	
ITHBOT	INDEX DEFINING LOWER BOUNDARY OF THERMOCLINE	
ITHUP	INDEX DEFINING UPPER BOUNDARY OF THERMOCLINE	
GR	TEMPERATURE GRADIENT	(°C/m)
DUM	DUMMY VARIABLE	
TAU	DIMENSIONLESS TIME USED IN DEEPENING ANALYSIS	
DRHO	MAXIMUM DENSITY DIFFERENCE AT GIVEN TIME	(kg/m ³)
IMAX	INDEX OF MAXIMUM TEMPERATURE GRADIENT	
TIME	ELAPSED TIME STARTING WHEN THERMOCLINE REACHED DIFFUSER	(sec)
IDEPN	CONTROL PARAMETER (IDEPN=1 DEEPENING DID NOT START) (IDEPN=2 DEEPENING STARTED ALREADY)	
HIN	THICKNESS OF INTERLAYER	(m)
HEP	THICKNESS OF EPILIMNION AT STAGNATION POINT	(m)
HIN	THICKNESS OF INTERLAYER AT STAGNATION POINT	(m)

TEP	TEMPERATURE OF UPPER LAYER IN TWO LAYER SYSTEM	(°C)
THY	TEMPERATURE OF LOWER LAYER IN TWO LAYER SYSTEM	(°C)
HEP0	THICKNESS OF UPPER LAYER IN TWO LAYER SYSTEM	(m)
HHY0	THICKNESS OF LOWER LAYER IN TWO LAYER SYSTEM	(m)
IA	INDEX OF THE LOWER BOUNDARY OF INTERLAYER	
IB	INDEX OF THE UPPER BOUNDARY OF INTERLAYER	
IDIF	INDEX OF SUBMERGENCE DEPTH OF DIFFUSER	
DTSIM	TIME STEP IN A GIVEN SEQUENCE	(sec)
TELAP	TIME ELAPSED	(sec)
HD	DISTANCE BETWEEN DIFFUSER AND BOTTOM OF RESERVOIR	(m)
H0	INITIAL DISTANCE BETWEEN THERMOCLINE AND DIFFUSER	(m)
AAVE	AVERAGE CROSS SECTION AREA IN REGION BELOW DIFFUSER	(m ²)
TIME0	TIME AT WHICH THERMOCLINE REACHED DIFFUSER'S DEPTH	(sec)
ZP	DEPTH AT WHICH FLOW RATE IN BUBBLE PLUME IS CALCULATED	(m)
QP	WATER FLOW RATE AT DEPTH ZP	(m ³ /s)
ICMAX	NUMBER OF ELEMENTS IN ZP AND QP ARRAYS	
TSIM	TIME STEP IN A GIVEN SEQUENCE	(sec)
NSL	PARAMETER DEFINING THE SIZE OF ARRAYS (CORRESPONDS TO MAIN PROGRAM)	
TA	TEMPERATURE OF I-TH LAYER	(°C)
ZA	DEPTH OF I-TH LAYER	(m)
DZ	THICKNESS OF I-TH LAYER	(m)
A	CROSS SECTIONAL AREA OF I-TH LAYER	(m ²)
VA	VOLUME OF I-TH LAYER	(m ³)
NLAY	NUMBER OF LAYERS IN A GIVEN SEQUENCE	
HTOT	TOTAL DEPTH	(m)

Subroutine: **NEARFLD**

RK	CONSTANT = 0.0725	
G	ACCELERATION DUE TO GRAVITY = 9.81	(m/s ²)
PI	CONSTANT = 3.14159	
RH0	PRESSURE HEAD (ATMOSPHERIC) AT THE WATER SURFACE	(m)
RDUB	BUBBLES SLIP VELOCITY	(m/s)
RE1	DUMMY VARIABLE	
RE2	DUMMY VARIABLE	
RWMIN	MINIMUM ERROR IN EVALUATION OF RADIUS OF STAGNATION POINT	
RSTEP	INCREMENT IN EVALUATION OF STAGNATION POINT RADIUS	(m)
T	DUMMY VARIABLE	
ISTART	STARTING INDEX IN LOOP TO EVALUATE STAGNATION POINT RADIUS	
RAD	STAGNATION POINT RADIUS AT GIVEN ITERATION	(m)
IEND	ENDING INDEX IN LOOP TO EVALUATE STAGNATION POINT RADIUS	
DRW	FORCE BALANCE ERROR AT GIVEN ITERATION	

JMIN.	INDEX OF THE ITERATION WITH MINIMUM FORCE BALANCE ERROR	
IREP.	INDEX CONTROLLING NUMBER OF REPETITION IN SEARCH FOR STAGNATION POINT RADIUS WITH MINIMUM ERROR	
LAST.	CONTROL INDEX IN SEARCH FOR STAGNATION POINT RADIUS WITH MINIMUM ERROR	
RSQ	DUMMY VARIABLE	
RDUM.	DUMMY VARIABLE	
RDUM6	DUMMY VARIABLE	
ISTAT	CONTROL INDEX IN SEARCH FOR STAGNATION POINT RADIUS WITH MINIMUM ERROR	
C	ENTRAINMENT COEFFICIENT FOR THE FLOW FROM EPILIMNION = 0.3	
QAIR	VOLUMETRIC AIR FLOW RATE UNDER ATMOSPHERIC CONDITIONS	(m ³ /s)
HDIFF	SUMBERGENCE DEPTH OF DIFFUSER	(m)
HEP	THICKNESS OF EPILIMNION AT STAGNATION POINT	(m)
HIN	THICKNESS OF INTERLAYER AT STAGNATION POINT	(m)
TEP	TEMPERATURE OF UPPER LAYER IN TWO LAYER SYSTEM	(°C)
THY	TEMPERATURE OF LOWER LAYER IN TWO LAYER SYSTEM	(°C)
HEP0	THICKNESS OF UPPER LAYER IN TWO LAYER SYSTEM	(m)
HHY0	THICKNESS OF LOWER LAYER IN TWO LAYER SYSTEM	(m)
RO	STAGNATION POINT RADIUS	(m)
RM	MOMENTUM COEFFICIENT	
RQW	WATER FLOW RATE ENTRAINED BY BUBBLE PLUME AT THE SURFACE	(m ³ /s)
RH	SUBMERGENCE DEPTH OF DIFFUSER	(m)
RTEP	TEMPERATURE OF UPPER LAYER IN TWO LAYER SYSTEM	(°C)
RTHY	TEMPERATURE OF LOWER LAYER IN TWO LAYER SYSTEM	(°C)
RHEP0	THICKNESS OF UPPER LAYER IN TWO LAYER SYSTEM	(m)
RHHY0	THICKNESS OF LOWER LAYER IN TWO LAYER SYSTEM	(m)
RQAIR	VOLUMETRIC AIR FLOW RATE UNDER ATMOSPHERIC CONDITIONS	(m ³ /s)
RHOE	WATER DENSITY IN UPPER LAYER IN TWO LAYER SYSTEM	(kg/m ³)
REIOH	WATER DENSITY IN LOWER LAYER IN TWO LAYER SYSTEM	(kg/m ³)
DRHOHE	DENSITY DIFFERENCE IN TWO LAYER SYSTEM	(kg/m ³)
RDUM1	DUMMY VARIABLE	
RDUM2	DUMMY VARIABLE	
RDUM5	DUMMY VARIABLE	
RAE	DIMENSIONLESS WATER FLOW RATE IN EPILIMNION	
RAH	DIMENSIONLESS WATER FLOW RATE IN HYPOLIMNION	
RHEP	THICKNESS OF EPILIMNION AT STAGNATION POINT	(m)
RHIN	THICKNESS OF INTERLAYER AT STAGNATION POINT	(m)

RFARF4	DUMMY VARIABLE	
RFN	NEARFIELD PRESSURE FORCE	(N)
C03	DUMMY VARIABLE	
RFARF5	DUMMY VARIABLE	
RZSTAR	DUMMY VARIABLE	
DRHH	DUMMY VARIABLE	
C04	DUMMY VARIABLE	
ART	DIMENSIONLESS RETURN FLOW RATE AT STAGNATION POINT	
RDQ	DUMMY VARIABLE	
C05	DUMMY VARIABLE	
KCON	INDEX	
RDUM3	DUMMY VARIABLE	
RFDP	FARFIELD OVERPRESSURE IMPACT	(N)
RDUM4	DUMMY VARIABLE	
RFARB	DUMMY VARIABLE	
RVE	MEAN VELOCITY IN EPILIMNION	(m/s)
RVH	MEAN VELOCITY IN HYPOLIMNION	(m/s)
RDZ	DUMMY VARIABLE	
CRAZ	DUMMY VARIABLE	
RFARF	DUMMY VARIABLE	
RVI	MEAN VELOCITY IN INTERLAYER	(m/s)
RHOI	INTERLAYER WATER DENSITY	(kg/m ³)
RCON	DUMMY VARIABLE	
KKCON	INDEX	
RUR	RADIAL VELOCITY	(m/s)
RHHY	THICKNESS OF HYPOLIMNION AT STAGNATION POINT	(m)
DRHOIE	DENSITY DIFFERENCE (INTERLAYER-EPILIMNION)	(kg/m ³)
RZO	THICKNESS OF THE SURFACE RADIAL JET	(m)
DRHOHI	DENSITY DIFFERENCE (HYPOLIMNION-INTERLAYER)	(kg/m ³)
RHEP0	THICKNESS OF UPPER LAYER IN TWO LAYER SYSTEM	(m)
RHHY0	THICKNESS OF LOWER LAYER IN TWO LAYER SYSTEM	(m)
RQAIR	VOLUMETRIC AIR FLOW RATE UNDER ATMOSPHERIC CONDITIONS	(m ³ /s)
RHOE	WATER DENSITY IN UPPER LAYER IN TWO LAYER WATER	(kg/m ³)
RHOH	WATER DENSITY IN LOWER LAYER IN TWO LAYER SYSTEM	(kg/m ³)
DRHOHE	DENSITY DIFFERENCE (HYPOLIMNION-EPILIMNION)	(kg/m ³)
RDUM1	DUMMY VARIABLE	
RDUM2	DUMMY VARIABLE	
RDUM5	DUMMY VARIABLE	
RAE	DIMENSIONLESS FLOW RATE IN EPILIMNION AT STAGNATION POINT	
RAH	DIMENSIONLESS FLOW RATE IN EPILIMNION AT STAGNATION POINT	
RHEP	THICKNESS OF EPILIMNION AT STAGNATION POINT	(m)
RHIN	THICKNESS OF INTERLAYER AT STAGNATION POINT	(m)
RDUM6	DUMMY VARIABLE	
ISTAT	CONTROL INDEX	
C	ENTRAINMENT COEFFICIENT FOR THE FLOW FROM EPILIMNION = 0.3	
ZP	DEPTH AT WHICH FLOW RATE IN BUBBLE PLUME IS CALCULATED	(m)
QP	WATER FLOW RATE AT DEPTH ZP	(m ³ /s)

ICMAX	NUMBER OF ELEMENTS IN ZP AND QP ARRAYS	
ROO	INITIAL STAGNATION POINT RADIUS	(m)
RM	MOMENTUM COEFFICIENT	
RQW	WATER FLOW RATE ENTRAINED BY BUBBLE PLUME AT THE SURFACE	(m ³ /s)
RH	SUBMERGENCE DEPTH OF DIFFUSER	(m)
RTEP	TEMPERATURE OF UPPER LAYER IN TWO LAYER SYSTEM	(°C)
RTHY	TEMPERATURE OF LOWER LAYER IN TWO LAYER SYSTEM	(°C)

subroutine: **FARFLD**

QE2	DUMMY VARIABLE	
HB	THICKNESS OF EPILIMNION IN FARFIELD	(m)
QINTER	INTERLAYER FLOW RATE	(m ³ /s)
TINTER	INTERLAYER WATER TEMPERATURE	(°C)
QL	ENTRAINED WATER FLOW RATE IN I-TH LAYER	(m ³ /s)
RDCF	DUMMY VARIABLE	
HHY	THICKNESS OF HYPOLIMNION IN FARFIELD	(m)
QHYP	WATER FLOW RATE IN HYPOLIMNION PER UNIT HEIGHT	(m ³ /s/m)
QEPI	WATER FLOW RATE IN EPILIMNION PER UNIT HEIGHT	(m ³ /s/m)
HIN	THICKNESS OF INTERLAYER IN FARFIELD	(m)
VRCP	DUMMY VARIABLE	(m)
QINT	WATER FLOW RATE IN INNER LAYER PER UNIT HEIGHT	(m ³ /s/m)
IA	INDEX OF THE LOWER BOUNDARY OF INTERLAYER	
IB	INDEX OF THE UPPER BOUNDARY OF INTERLAYER	
IDIF	INDEX OF SUBMERGENCE DEPTH OF DIFFUSER	
DTSIM	TIME STEP IN A GIVEN SEQUENCE	(sec)
HMK	DIFFUSION COEFFICIENT IN FARFIELD DUE TO AIR MIXING	(m ² /s)
T	TEMPERATURE OF I-TH LAYER	(°C)
ZA . .	DEPTH OF I-TH LAYER	(m)
DZ . .	THICKNESS OF I-TH LAYER	(m)
A . .	CROSS SECTIONAL AREA OF I-TH LAYER	(m ²)
VA . .	VOLUME OF I-TH LAYER	(m ³)
NLAY.	NUMBER OF LAYERS IN A GIVEN SEQUENCE	
HTOT.	TOTAL DEPTH	(m)
HDIFF	SUMBERGENCE DEPTH OF DIFFUSER	(m)
NDAYC	NUMBER OF TIME UNITS ELAPSED	
QEO .	FLOW RATE IN EPILIMNION AT STAGNATION POINT	(m ³ /s)
QHO .	FLOW RATE IN HYPOLIMNION AT STAGNATION POINT	(m ³ /s)
HEP .	THICKNESS OF EPILIMNION AT STAGNATION POINT	
HIN .	THICKNESS OF INTERLAYER AT STAGNATION POINT	
NSL .	PARAMETER DEFINING THE SIZE OF ARRAYS (CORRESPONDS TO MAIN PROGRAM)	

function: **IAB**

HH . .	DEPTH	(m)
Z . .	DEPTH OF I-TH LAYER	(m)
DZ . .	THICKNESS OF I-TH LAYER	(m)

NLAY. NUMBER OF LAYERS IN A GIVEN SEQUENCE
 NSL. PARAMETER DEFINING THE SIZE OF ARRAYS
 (CORRESPONDS TO MAIN PROGRAM)

subroutine: **SUBRTN**

CONFM CONVERSION FACTOR FROM FEET TO METER
 CKAFM3 CONVERSION FACTOR FROM KACRE FEET TO CUBIC METERS
 VCNEW CUMULATIVE VOLUME IN AIRMIX AFTER MIXING (m³)
 DUM1 DUMMY VARIABLE
 DUM2 DUMMY VARIABLE
 DUM3 DUMMY VARIABLE
 TL.. TEMPORARY TEMPERATURE FIELD (°C)
 ZN.. DEPTH IN FARFIELD AFTER AIR MIXING (m)
 IDONE CONTROL INDEX
 ATOP. CROSS SECTIONAL AREA AT TOP OF I-TH LAYER (m²)
 VCOLD CUMULATIVE VOLUME IN AIRMIX BEFORE MIXING (m³)
 DELZ. LAYER THICKNESS FROM THE MAIN PROGRAM (feet)
 DELZM LAYER THICKNESS IN METERS (m)
 DTSIM TIME STEP IN A GIVEN SEQUENCE (sec)
 TEMP. WATER TEMPERATURE FROM THE MAIN PROGRAM (°C)
 VOL. VOLUME OF I-TH LAYER FROM MAIN PROGRAM (Kacre feet)
 HMK. DIFFUSION COEFFICIENT IN FARFIELD DUE TO AIR MIXING (m²/s)
 AK.. COEFFICIENT IN TDMA SOLUTION OF DIFFUSION EQUATION
 BK.. COEFFICIENT IN TDMA SOLUTION OF DIFFUSION EQUATION
 CK.. COEFFICIENT IN TDMA SOLUTION OF DIFFUSION EQUATION
 DK.. COEFFICIENT IN TDMA SOLUTION OF DIFFUSION EQUATION
 DTSIM. TIME STEP IN A GIVEN SEQUENCE (sec)
 TA. TEMPERATURE OF I-TH LAYER (°C)
 ZA. DEPTH OF I-TH LAYER (m)
 DZ. THICKNESS OF I-TH LAYER (m)
 A.. CROSS SECTIONAL AREA OF I-TH LAYER (m²)
 VA.. VOLUME OF I-TH LAYER (m³)
 NLAY. NUMBER OF LAYERS IN A GIVEN SEQUENCE
 HTOT. TOTAL DEPTH (m)
 HDIFF SUMBERGENCE DEPTH OF DIFFUSER (m)
 NDAYC NUMBER OF TIME UNITS ELAPSED
 PDNUM NUMBER OF POINT DIFFUSERS
 NDAYC NUMBER OF TIME UNITS ELAPSED
 NSL1. PARAMETER DEFINING THE SIZE OF ARRAYS (=NSL+1)
 NSL. PARAMETER DEFINING THE SIZE OF ARRAYS
 (CORRESPONDS TO MAIN PROGRAM)

subroutine: **SOLVE**

NLAY. NUMBER OF LAYERS IN A GIVEN SEQUENCE
 VAR.. GENERAL VARIABLE
 TT.. DUMMY VARIABLE
 TX.. DUMMY VARIABLE

AK.. COEFFICIENT IN TDMA SOLUTION OF DIFFUSION EQUATION
BK.. COEFFICIENT IN TDMA SOLUTION OF DIFFUSION EQUATION
CK.. COEFFICIENT IN TDMA SOLUTION OF DIFFUSION EQUATION
DK.. COEFFICIENT IN TDMA SOLUTION OF DIFFUSION EQUATION
NSL. PARAMETER DEFINING THE SIZE OF ARRAYS (CORRESPONDS TO MAIN PROGRAM)

Subroutine: **BPLUME**

HDIFF SUMBERGENCE DEPTH OF DIFFUSER (m)
QAIR. VOLUMETRIC AIR FLOW RATE UNDER ATMOSPHERIC CONDITIONS (m³/s)
ISTAT CONTROL INDEX (= 1 MEANS THAT CONVERGENCE WAS NOT OBTAINED)
AZC . DEPTH AT WHICH FLOW RATE IN BUBBLE PLUME IS CALCULATED (m)
AQC. . WATER FLOW RATE AT DEPTH ZP (m³/s)
ZP. . DEPTH AT WHICH FLOW RATE IN BUBBLE PLUME IS CALCULATED (m)
QP. . WATER FLOW RATE AT DEPTH ZP (m³/s)
ICMAX NUMBER OF ELEMENTS IN ZP AND QP ARRAYS

subroutine: **STRTS**

ISTAT CONTROL INDEX (= 1 MEANS THAT CONVERGENCE WAS NOT OBTAINED)
HDIF SUMBERGENCE DEPTH OF DIFFUSER (m)
QGAS. VOLUMETRIC AIR FLOW RATE UNDER ATMOSPHERIC CONDITIONS (m³/s)
B. BUBBLE PLUME WIDTH (m)
Q1 WATER FLOW RATE AT HEIGHT Z1 (m³/s)
NITER NUMBER OF ITERATIONS
Q2. WATER FLOW RATE AT HEIGHT Z2 (m³/s)
MSPT. PARAMETER USED IN DEFINING NUMBER OF ITERATIONS
D.. DIAMETER OF DIFFUSER (m)
BC.. PLUME WIDTH AT HEIGHT Z2 (m)
POINT INDEX CONTROLLING A NUMBER OF ITERATIONS
NSTEP INDEX CONTROLLING A NUMBER OF ITERATIONS
IC. INDEX
S.. MEAN PLUME DENSITY AT HEIGHT Z2 (kg/m³)
U.. PLUME CENTERLINE VELOCITY (m/s)
SC.. MEAN PLUME DENSITY AT HEIGHT Z2 (kg/m³)
BU. . BUBBLE WEBER NUMBER
UB. . TEMPORARY VARIABLE
UC. . PLUME CENTERLINE VELOCITY (m/s)
UBE . TEMPORARY VARIABLE
DZ. . INCREMENT IN Z (m)
DZA . INCREMENT IN Z (m)
NIT. . NUMBER OF ITERATIONS
IZFE. . INDEX FOR THE ZONE OF FLOW ESTABLISHMENT
ZEND. TOTAL PLUME LENGTH (m)

SIGMA	SURFACE TENSION OF WATER = 0.0736	(N/m)
MGPT.	INDEX CONTROLLING A NUMBER OF ITERATIONS	
ICMAX	MAXIMUM NUMBER OF STORED FLOW RATES QC	
DW. .	WATER DENSITY = 1000	(kg/m ³)
G . . .	ACCELERATION DUE TO GRAVITY = 9.81	(m/s ²)
HT. .	ATMOSPHERIC PRESSURE HEAD = 10.2	(m)
HB. .	PRESSURE HEAD AT THE LEVEL OF GAS RELEASE	(m)
QGT .	GAS FLOW RATE AT ATMOSPHERIC PRESSURE	(m ³ /s)
DGT .	GAS DENSITY AT. ATMOSPHERIC PRESSURE = 1.25	(kg/m ³)
US. .	BUBBLE RELATIVE VELOCITY = 0.25	(m/s)
GAM .	GAMA COEFFICIENT	
BU	BUBBLE PLUME WEBER NUMBER	
ALP .	ALPHA COEFFICIENT	
AML .	LAMBDA COEFFICIENT	
Z1. .	ELEVATION ABOVE DIFFUSER	(m)
Z2	ELEVATION ABOVE DIFFUSER	(m)
S1. .	DENSITY DEFICIT AT ELEVATION Z1	(kg/m ³)
U0.	GAS VELOCITY AT DIFFUSER	(m/s)
PI. .	CONSTANT = 3.14159	
ZC. .	ELEVATION WHERE WATER FLOW RATES ARE STORED	(m)
QC. .	WATER FLOW RATE AT ELEVATIONS ZC	(m ³ /s)

Appendix C

Input Files Used for Simulation of Destratification

```

TITLE      *** LAKE CALHOUN 1972***
TITLE
TITLE      *****          CE-THERM          *****
TITLE
TITLE
JOB        217  250  24  24  217  72
MODE      NORMAL  PORT SPECIFY  YES
PHYS1     1   40  45.0  93.0  .06  3.3-09  1.2E-09  285.
PHYS2     1470  0.50  2.00
PHYS2+    0.625  0.625  0.625  0.625  0.625  0.625  0.625  0.625  0.625
PHYS2+    0.625  0.625  0.625  0.625  0.625  0.625  0.625  0.625  0.625
PHYS2+    0.625  0.625  0.625  0.625  0.625  0.625  0.625  0.625  0.625
PHYS2+    0.625  0.625  0.625  0.625  0.625  0.625  0.625  0.625  0.625
PHYS2+    0.625  0.625  0.625  0.625
OUTLET    1
PHYS3     3.00  4.31  4.31
CURVE     POWER
AREAC     4966.498  1.81259
WIDTHC    79.52094  0.90630
MIXING    0.5  .30  1.0-08  1.0-02  .1
LIGHT     1.0  0.60  0.01
SSETL     .05  30.  40.  .003  .005
INIT0     25
INIT2     0.   6.4  0   0   0
INIT2     1.5  6.4  0   0   0
INIT2     2.5  6.5  0   0   0
INIT2     3.5  6.5  0   0   0
INIT2     4.5  6.6  0   0   0
INIT2     5.5  6.7  0   0   0
INIT2     6.5  6.73  0   0   0
INIT2     7.5  6.75  0   0   0
INIT2     8.5  6.85  0   0   0
INIT2     9.5  7.00  0   0   0
INIT2     10.5  7.18  0   0   0
INIT2     11.5  7.32  0   0   0
INIT2     12.5  7.55  0   0   0
INIT2     13.5  7.75  0   0   0

```

INIT2	14.5	8.05	0	0	0	
INIT2	15.5	8.65	0	0	0	
INIT2	16.5	9.40	0	0	0	
INIT2	17.5	10.8	0	0	0	
INIT2	18.5	13.9	0	0	0	
INIT2	19.5	18.6	0	0	0	
INIT2	20.5	21.8	0	0	0	
INIT2	21.5	22.45	0	0	0	
INIT2	22.5	22.5	0	0	0	
INIT2	23.5	22.5	0	0	0	
INIT2	24.5	22.5	0	0	0	
FILES	PLTWC R1PLT04 R1PLT11 R1PLT12					
FILID	TEST DATA SET FOR CALHOUN 1971					
WEATH1	24	41				
W2	8 4	0.1	17.78	9.44	1000.	9.34
W2	8 5	1.0	18.89	14.44	1000.	15.94
W2	8 6	0.9	17.22	13.89	1000.	18.35
W2	8 7	0.7	13.89	10.00	1000.	11.59
W2	8 8	0.9	14.44	10.00	1000.	20.77
W2	8 9	0.8	14.44	8.89	1000.	8.53
W2	8 10	0.9	18.33	13.33	1000.	19.00
W2	8 11	0.5	22.78	17.78	1000.	7.25
W2	8 12	0.0	21.67	16.11	1000.	8.05
W2	8 13	0.7	23.33	19.44	1000.	10.14
W2	8 14	0.4	26.11	20.56	1000.	12.72
W2	8 15	0.6	26.11	21.11	1000.	18.84
W2	8 16	0.3	30.56	20.56	1000.	23.67
W2	8 17	0.2	29.44	21.67	1000.	10.63
W2	8 18	0.6	28.89	19.44	1000.	15.13
W2	8 19	0.4	27.22	21.11	1000.	15.30
W2	8 20	0.3	29.44	21.11	1000.	18.03
W2	8 21	0.9	24.44	20.00	1000.	15.30
W2	8 22	1.0	17.78	12.78	1000.	22.54
W2	8 23	1.0	14.44	10.56	1000.	15.78
W2	8 24	1.0	13.89	11.67	1000.	8.37
W2	8 25	1.0	16.67	14.44	1000.	12.72
W2	8 26	1.0	17.22	15.56	1000.	14.81
W2	8 27	0.7	21.67	15.56	1000.	11.43
W2	8 28	0.0	23.33	16.67	1000.	3.54
W2	8 29	0.0	23.89	18.33	1000.	9.34
W2	8 30	0.9	24.44	17.78	1000.	15.78
W2	8 31	0.9	20.00	15.56	1000.	19.64
W2	9 1	0.9	15.00	10.00	1000.	9.50
W2	9 2	0.3	14.44	6.67	1000.	6.44
W2	9 3	0.9	12.78	9.44	1000.	7.89
W2	9 4	0.7	16.67	12.22	1000.	10.63
W2	9 5	0.5	16.67	10.00	1000.	9.98
W2	9 6	0.9	18.89	16.11	1000.	22.70
W2	9 7	1.0	12.78	11.11	1000.	10.63
W2	9 8	0.0	12.78	7.22	1000.	6.44
W2	9 9	0.4	15.56	10.00	1000.	14.65
W2	9 10	1.0	18.89	14.44	1000.	21.09
W2	9 11	0.9	19.44	15.00	1000.	9.50
W2	9 12	1.0	17.22	15.56	1000.	11.11
W2	9 13	1.0	17.22	15.00	1000.	11.75


```

WQ SSOL 168 0
VERIFY1 YES
VERIFY2 8
NVRFY 218 18 23.8 6.52 22.5 6.50 20.7 6.64 18.8 6.74
17.5 7.52 15.6 7.93 14.4 8.34 13.2 9.14
12.0 9.62 10.7 10.29 9.4 11.98 8.7 13.45
6.8 14.88 5.6 17.96 5.0 19.00 3.1 22.80
2.4 22.81 0.6 22.78
NVRFY 220 21 18.0 6.94 21.9 6.97 20.0 7.31 19.4 8.00
18.1 8.63 17.5 8.90 16.3 9.55 15.0 9.91
14.5 10.63 13.1 11.01 12.6 11.65 11.2 11.93
10.1 12.47 9.4 13.36 8.1 13.99 7.5 14.19
6.2 14.94 5.0 15.98 4.3 16.25 2.4 20.06
1.8 20.10
NVRFY 222 24 23.7 7.27 22.4 7.31 21.9 7.31 21.3 7.30
19.9 7.48 18.8 7.99 18.1 9.76 16.9 10.00
16.2 10.49 14.9 11.03 13.7 11.53 13.1 11.91
11.8 12.10 11.2 12.69 9.9 13.07 8.7 13.38
8.1 13.98 6.8 14.22 6.2 15.08 4.9 15.18
3.7 15.53 3.1 16.11 1.8 17.74 1.2 18.01
NVRFY 227 19 23.7 7.93 22.6 8.38 20.6 10.98 18.8 12.83
17.4 13.83 15.6 13.99 15.0 14.37 13.8 14.58
12.5 14.78 11.9 14.80 10.6 14.95 9.4 15.12
8.7 15.41 6.8 15.64 5.6 15.89 4.9 16.44
3.1 17.38 2.4 20.10 0.6 24.57
NVRFY 230 18 23.8 8.18 22.5 8.67 20.6 10.06 18.8 14.06
17.4 14.42 15.6 14.85 14.4 15.07 13.1 15.37
11.9 15.64 10.6 15.93 9.3 16.01 8.8 16.12
6.8 16.39 5.6 16.80 4.9 17.54 3.1 19.44
2.4 21.24 0.5 25.63
NVRFY 231 14 23.8 8.42 21.9 9.00 20.6 10.80 20.0 13.97
16.3 14.66 13.7 14.94 11.3 15.30 9.3 16.12
6.8 16.89 5.6 17.03 5.0 17.52 3.8 19.08
2.5 20.42 0.6 25.49
NVRFY 235 16 23.8 9.05 22.5 9.54 21.3 10.11 19.9 13.53
16.9 15.20 15.1 15.99 12.6 16.23 11.3 16.45
10.1 16.81 8.7 16.87 6.8 17.43 5.0 17.90
4.3 18.74 3.1 19.19 2.4 20.05 0.5 22.04
NVRFY 242 18 23.7 8.99 22.5 9.01 21.9 9.45 20.7 10.23
20.0 12.20 18.8 15.89 17.5 16.17 16.9 16.83
14.5 17.09 11.9 17.18 9.4 17.32 7.4 17.66
5.6 17.84 5.0 17.98 3.7 18.00 2.4 18.67
1.9 19.08 0.6 21.88

```

Appendix D

Output File From Air Mixing Routine

- for CE-QUAL-R1 version

*AIR FLOW RATE PER DIFFUSER =0.0590 (M3/S)
*DEPTH OF DIFFUSER =19.00 (M)
*NUMBER OF DIFFUSERS =1.00

NO.	MIXING (%)	Qi (m3/s)
0	0.0	0.0
1	15.7	18.9
2	28.3	19.0
3	43.1	18.3
4	55.3	17.8
5	69.3	16.5
6	75.7	16.8
7	80.6	16.6
8	82.6	16.9
9	81.3	16.8
10	77.4	16.8
11	75.4	16.8
12	73.7	14.1
13	71.2	15.4
14	66.9	14.5
15	61.2	14.2
16	59.1	13.9
17	59.4	14.5
18	58.8	14.5
19	69.8	15.3
20	78.9	16.6
21	86.6	17.5
22	92.6	19.3
23	95.9	17.7
24	97.4	15.8
25	97.6	14.2

26	93.7	15.0
27	89.0	16.3
28	91.1	20.2
29	93.4	24.0
30	95.9	16.9
31	98.2	13.7

TEMPERATURE DIFFERENCE OVER DIFFUSER DEPTH DROPPED
UNDER 1 DEG C

** AIR IS SHUT OFF **

REPORT DOCUMENTATION PAGE

Form Approved
OMB No. 0704-0188

Public reporting burden for this collection of information is estimated to average 1 hour per response, including the time for reviewing instructions, searching existing data sources, gathering and maintaining the data needed, and completing and reviewing the collection of information. Send comments regarding this burden estimate or any other aspect of this collection of information, including suggestions for reducing this burden, to Washington Headquarters Services, Directorate for Information Operations and Reports, 1215 Jefferson Davis Highway, Suite 1204, Arlington, VA 22202-4302, and to the Office of Management and Budget, Paperwork Reduction Project (0704-0188), Washington, DC 20503.

1. AGENCY USE ONLY (Leave blank)	2. REPORT DATE June 1994	3. REPORT TYPE AND DATES COVERED Final report	
4. TITLE AND SUBTITLE Destratification Induced by Bubble Plumes		5. FUNDING NUMBERS	
6. AUTHOR(S) Kreshimir Zic, Hienz G. Stefan, Herman O. Turner, ed., Steven C. Wilhelms, ed.		8. PERFORMING ORGANIZATION REPORT NUMBER	
7. PERFORMING ORGANIZATION NAME(S) AND ADDRESS(ES) St. Anthony Falls Hydraulic Laboratory, Department of Civil and Mineral Engineering, University of Minnesota, 3rd Avenue at Mississippi River, S.E., Minneapolis, MN 55414; U.S. Army Engineer Waterways Experiment Station, 3909 Halls Ferry Road, Vicksburg, MS 39180-6199		10. SPONSORING/MONITORING AGENCY REPORT NUMBER Technical Report W-94-3	
9. SPONSORING/MONITORING AGENCY NAME(S) AND ADDRESS(ES) U.S. Army Corps of Engineers, Washington, DC 20314-1000		11. SUPPLEMENTARY NOTES Available from National Technical Information Service, 5285 Port Royal Road, Springfield, VA 22161.	
12a. DISTRIBUTION/AVAILABILITY STATEMENT Approved for public release; distribution is unlimited.		12b. DISTRIBUTION CODE	
13. ABSTRACT (Maximum 200 words) Destratification is an alternative for improving the overall quality, particularly dissolved oxygen content, of a stratified reservoir. Pneumatic systems have been used most often for providing the energy needed to destratify a water body. However, there are no means to evaluate the long-term operation of a destratification system. Under contract, the St. Anthony Falls Hydraulic Laboratory, University of Minnesota, developed a subroutine entitled "BUBBLES" that simulates the destratification of a lake or reservoir by an air bubble diffuser. This subroutine was added to CE-THERM-R1 and used to account for mixing that occurs in a lake or reservoir caused by a pneumatic destratification system. CE-THERM-R1 contains the thermal analysis portion of CE-QUAL-R1 and is used to simulate the water and heat budgets of a water body. This report describes the development of BUBBLES and its incorporation into CE-THERM-R1. In BUBBLES, the reservoir is divided into a near field and a far field. The near-field model includes the bubble plume and the flow in its vicinity. The far-field model treats the rest of the reservoir and considers the flow from the plume toward the lake and from the lake toward the plume. The far-field model is coupled with CE-THERM-R1 to simulate water and heat budgets of the water body.			
14. SUBJECT TERMS Bubble plume Pneumatic Destratification Reservoir Diffuser Water quality Lake		15. NUMBER OF PAGES 64	
17. SECURITY CLASSIFICATION OF REPORT UNCLASSIFIED		16. PRICE CODE	
18. SECURITY CLASSIFICATION OF THIS PAGE UNCLASSIFIED	19. SECURITY CLASSIFICATION OF ABSTRACT	20. LIMITATION OF ABSTRACT	